Transportation Research Part C 142 (2022) 103777

Contents lists available at ScienceDirect

Transportation Research Part C

journal homepage: www.elsevier.com/locate/trc

Spatial pricing of ride-sourcing services in a congested transportation network

Fatima Afifah, Zhaomiao Guo *

Department of Civil, Environmental and Construction Engineering, Resilient, Intelligent, and Sustainable Energy Systems Center, University of Central Florida, FL 32766, United States of America

ARTICLE INFO

Keywords:
Ride-sourcing
Transportation network company (TNC)
Dynamic pricing
Traffic equilibrium
Stackelberg game

ABSTRACT

We investigate the impacts of spatial pricing for ride-sourcing services in a Stackelberg framework considering traffic congestion. In the lower level, we use combined distribution and assignment approaches to explicitly capture the interactions between drivers' relocation, riders' mode choice, and all travelers' routing decisions. In the upper level, a single transportation network company (TNC) determines spatial pricing strategies to minimize imbalance in a two-sided market. We show the existence of the optimal pricing strategies for locational imbalance minimization, and propose effective algorithms with reliable convergence properties. Furthermore, the optimal pricing is unique and can be solved in a convex reformulation when waiting time is small compared to travel time. We conduct numerical experiments on different scales of transportation networks with different TNC objectives to generate policy insights on how spatial pricing could impact transportation systems.

1. Introduction

Since the first introduction of UBER services in 2010, ride-sourcing has become an encouraging new form of mobility. Transportation network companies (TNCs), also known as ride-sourcing companies, serve as both platform providers and operators, promising to increase the reliability and efficiency of point-to-point transportation. Dynamic pricing[1] is one of TNCs' key operational techniques to improve locational supply–demand balance in real-time. Conceptually, dynamic pricing sets a surge multiplier (SM) for each predefined geographic area, which dynamically raises (or reduces) the base trip fare when locational demand is higher (or lower) than available supply until demand and supply are balanced[2]. While conceptually appealing, dynamic pricing receives critiques over the past years due to the opaque of pricing algorithm and concerns that TNCs may surge unnecessarily high or more frequently to exploit customers in an oligopolistic setting (Zha et al., 2018a).

Determining optimal pricing strategies may be challenging due to spatio-temporal couplings and potential conflicts of interest between the society and TNCs. On one hand, dynamic pricing tries to balance supply and demand both in time and in space, but most research attention has been paid to the temporal aspect (Bimpikis et al., 2019). Because pricing information (i.e., SM, base trip

* Correspondence to: 4353 Scorpius Street, Orlando, FL 32816-0120, United States of America.
E-mail address: guo@ucf.edu (Z. Guo).

[1] E.g., Uber surge pricing, Lyft prime time charges, and Didi Chuxing's dynamic pricing.

[2] In reality, prices for rides are dynamically calculated based on a variety of factors including route, time of day, ride type, number of available drivers, current demand for rides, and any local fees or surcharges. While the actual pricing algorithm is unknown to the public, Chen et al. (2015) reverse engineer the pricing strategies using high-resolution UBER data.

https://doi.org/10.1016/j.trc.2022.103777
Received 11 August 2021; Received in revised form 20 June 2022; Accepted 23 June 2022
Available online 15 July 2022

fare, etc.) is revealed to both demand and supply markets, which are interconnected through a transportation network, prices at one location affect services at all other locations potentially. In practice, TNCs also benefit from using spatial prices to account for long-term predictable unbalanced demand patterns (Bimpikis et al., 2019). Studying dynamic pricing from a network perspective is beneficial for both societal welfare and TNCs' mission. On the other hand, while TNCs are typically profit-driven, optimal prices for TNCs themselves may not be optimal for the whole society, which includes riders, drivers, and other transportation users. Better understanding the impact of TNCs' pricing decisions on system welfare is critical to generate planning and regulation insights for policymakers.

Although the current flow share of ride-sourcing traffic is low, several studies have found that ride-sourcing has a negative impact on traffic congestion. For example, using ride-sourcing data, Qian et al. (2020) showed that increased demand of ride-sourcing is a major cause of New York City's traffic congestion. A similar study by Castiglione et al. (2018) reported that congestion increased by 50% in San Francisco in a few years because of ride-sourcing services. As a result, several cities, such as NYC (NYCTLC, 2019) and Chicago (Pierog, 2019), have now imposed congestion surcharges on those services in an effort to alleviate congestion. Beojone and Geroliminis (2021) investigated the impact of ride-sourcing services on traffic congestion using Chinese ride-sourcing data and revealed that although a larger fleet size reduces waiting time, it intensifies congestion. Additionally, studies have found that young people have an inclination towards ride-sourcing services than to own private vehicles (Alemi et al., 2018; Dzisi et al., 2020), which will further increase the market share of ride-sourcing in the future. Given these circumstances, it is imperative to investigate the effects of ride-sourcing on traffic congestion.

In this paper, we investigate the spatial dimension of surge pricing while considering traffic congestion during the peak period. We analyze the impacts of spatial pricing for ride-sourcing services in an interconnected transportation network using a Stackelberg framework. In the lower level, we explicitly capture the interactions between drivers' relocation, riders' mode choice, and all travelers' routing decisions. In the upper level, a single TNC provider determines spatial pricing strategies to fulfill its objective in two-sided markets. The main contribution of this work is twofold. First, we explicitly consider the relocation of drivers and transportation congestion, which not only captures the ride-sourcing behaviors more accurately but also allows for systematic analyses of the impacts of spatial pricing on transportation efficiency. Second, while optimal spatial pricing problems are challenging to solve due to a bi-level structure, we propose effective computational algorithms, with rigorous analyses on the existence, uniqueness, and convergence of the optimal solutions.

The remainder of this paper is organized as follows. Section 2 reviews the relevant literature on dynamic pricing in the ride-sourcing context. Section 3 and Section 4 propose the formulations and algorithms, respectively. We test the models and solution approaches using different scales of transportation systems in Section 5. Section 6 concludes the paper with the main research findings and future research directions.

2. Literature review

According to SAE international (2018), ride-sourcing is defined as "prearranged and on-demand transportation services for compensation in which drivers and passengers connect via digital applications". This definition includes a broad range of mobility modes. In this paper, we focus on TNCs for automobiles.

As one of the key operational strategies, ride-sourcing pricing has attracted increasing attention from the various research communities, including transportation (e.g., (Zha et al., 2018a,b)), economics (e.g., (Chen and Sheldon, 2016; Bimpikis et al., 2019)), management science (e.g., (Guda and Subramanian, 2019)), and computer science (e.g., (Chen et al., 2015)). In addition, some studies on ride-sourcing modeling are closely related to research on taxi (e.g., (Yang and Wong, 1998; Lagos, 2000; Yang et al., 2010; Yang and Yang, 2011; He et al., 2018)) and two-sided marketplace (e.g., (Rochet and Tirole, 2006; Rysman, 2009; Hu et al., 2021)). Given the focus of this paper is on the impacts of spatial pricing on transportation congestion, we focus on the ride-sourcing pricing issues from a transportation perspective, with references to other domains as needed.

The impacts of dynamics pricing on ride-sourcing driver supply are still inconclusive. The first conjecture, denoted as income-target theory, is that drivers quit driving once a daily income target is reached. This theory is pioneered by Camerer et al. (1997), who found negative wage elasticity of cabdriver supply in New York City. In contrast, the second conjecture, denoted as the neoclassical theory (Farber, 2005), suggests that cabdrivers are greedy for higher income, and cabdrivers supply has a positive wage rate elasticity. Farber (2005) also pointed out that the differences between income-target theory and neoclassical theory are in the conception and measurement of the daily wage rate. Chen and Sheldon (2016) provided empirical evidence for neoclassical theory using high-resolution UBER data. The coexistence of these two competing theories may explain the empirical evidence that the effect of dynamic pricing on UBER drivers' supply is limited (Chen et al., 2015). Zha et al. (2018a) proposed a bi-level modeling framework, with lower-level equilibrium considering both income-target theory and neoclassical theory, and find that compared to static pricing, surge pricing leads to higher revenue for both the platform and drivers, but lower customer surplus during highly surged periods. The majority of these studies focus on the temporal dimension of dynamic pricing without considering spatial linkages between driver availability and traffic congestion. In this paper, due to the inconclusive impacts of dynamic pricing on driver supply, we assume that total driver supply is inelastic to spatial pricing, but drivers will respond to spatial pricing by choosing their service location.

Another school of literature investigates the potential value of dynamic pricing on ride-sourcing systems (Banerjee et al., 2015; Cachon et al., 2017; Castillo et al., 2017; Taylor, 2018; Gurvich et al., 2019). Banerjee et al. (2015) adopted a queueing-theoretical approach and find that dynamic pricing only outperforms static pricing when TNCs have imperfect knowledge of system parameters. Although network model is presented, the pricing policies only depend on the number of idle drivers at individual locations. Castillo

et al. (2017) considered the problem of "wild goose chase" when the price is set too low, and find that dynamic pricing can avoid this issue and maintain prices within a reasonable range. In contrast, in a deterministic setting, Zha et al. (2018b) adopted a geometric matching framework and find that dynamic pricing may still set price higher than the societal efficient level. However, idle vehicle relocation behaviors is not considered in (Zha et al., 2018b). Karamanis et al. (2018) explored the impact of dynamic pricing for autonomous vehicles in a one-sided market for private and shared rides in both monopoly and duopoly structure. Nourinejad and Ramezani (2020) investigated TNC's profit, driver's wage and rider's fare under different pricing strategies in a non-equilibrium two-sided market with pricing determined exogenously. Most of these studies focus on temporal aspects and do not consider traffic equilibrium and transportation congestion.

Bimpikis et al. (2019) are among the first to consider the spatial dimension of ride-sourcing pricing, by modeling whether and where drivers will join the platform, and where to relocate themselves when they are idle. Bimpikis et al. (2019) found that spatial pricing contributes to balance supply and demand, and more balanced demand patterns lead to higher profits and higher consumer surplus, simultaneously. However, the equilibrium formulation in (Bimpikis et al., 2019) is indeterminate and the conclusion is, therefore, best seen as an ideal bound (Zha et al., 2018b). In addition, since Bimpikis et al. (2019) mainly focused on the equilibrium of ride-sourcing services rather than traffic equilibrium, transportation topology and congestion effects are ignored. Similarly, Tang et al. (2022) examined long-term spatial pricing strategies based on long-term interaction between drivers and riders in different zones, but transportation network congestion effects are not considered. To optimize spatial–temporal pricing, Chen et al. (2021) proposed a reinforcement learning approach and shows that TNC's profit increases with dynamic pricing in real-world situations. Battifarano and Qian (2019) proposed a data-driven framework to predict surge multipliers in real-time. These studies do not aim to analytically explain the interaction between different components in ride-sourcing systems.

The congestion effect of ride-sourcing services in transportation networks is a relatively new research topic and, thus, less explored. Nie (2017) has indicated the concerns of ride-sourcing services on worsening the traffic congestion. A more recent work by Ban et al. (2019) using general equilibrium model to formulate the multi-agent interactions in an e-hailing system, has explicitly modeled traffic congestion under path independent free-flow travel time assumption. However, pricing is treated as exogenous parameters and not a focus in (Ban et al., 2019). Beojone and Geroliminis (2021) investigated the impact of ride-sourcing services on traffic congestion using agent-based modeling. The study reveals larger fleet size reduces waiting time but increases congestion thereby adds more to total travel time. Vignon et al. (2021) investigated the impact of both solo and pooling ride-sourcing services on traffic congestion, which provide crucial policy insights for regulating ride-sourcing services effectively. Nevertheless, these studies do not address the impact of spatial/dynamic pricing on ride-sourcing services under congested network conditions. Li et al. (2021b) proposed a network market equilibrium model to investigate the optimal spatial pricing for a ride-sourcing platform to maximize profits under different congestion pricing policies. However, the resulting model is non-convex and the global optimal is not guaranteed. We aim to fill this gap by proposing a mathematical tractable modeling framework for spatial pricing considering traffic equilibrium in a congested transportation network.

3. Methodologies

In this section, we present mathematical models for ride-sourcing systems in two cases: (1) ignoring waiting time (Section 3.1), and (2) considering waiting time (Section 3.2). The waiting time used in this paper is defined as follows. For a rider, waiting time is the duration between a request being made and the rider being picked up. For a driver, waiting time is the duration between the time when the driver arrives at the desired service location waiting for ride requests and the time when the driver picks up a rider. Based on this definition, the waiting time includes matching time and pick up time. This definition is consistent with existing ride-sourcing literature (e.g., (Yang and Yang, 2011; Zha et al., 2016)).

3.1. Mathematical modeling: Ignoring waiting time

Firstly, we ignore the impacts of waiting time on the behaviors of drivers and riders. This assumption will be relaxed in Section 3.2. Models ignoring waiting time are appropriate when waiting time is an insignificant factor for drivers' and riders' decision making. For example, for long-term transportation planning problems with congestion, relocation/travel time can significantly exceed waiting time. In addition, travelers may be able to request rides earlier than their intended departure time, so that ride request decisions are less sensitive to waiting time.

3.1.1. Traffic modeling

Denote a transportation network by a directed graph $\mathcal{G} = (\mathcal{N}, \mathcal{A})$, where $\mathcal{N}$ is the set of nodes (indexed by n) and $\mathcal{A}$ is the set of links (indexed by a). The service area we consider is a metropolitan area where ride-sourcing demand and supply are aggregated in predefined zones (e.g., census tracts or traffic analysis zones), represented by nodes. A link is a sequence of roads that connects two nodes. Given driver node set $\mathcal{R}$ ($\subset \mathcal{N}$) and rider node set $\mathcal{S}$ ($\subset \mathcal{N}$), drivers will relocate from r ($\in \mathcal{R}$) to s ($\in \mathcal{S}$) to provide ride-sourcing services depends on spatial pricing. In other words, there are two "origins" used in this paper. A driver's origin, denoted as r, is the driver's current location before he/she makes relocation; a rider's origin or a driver's relocation destination, denoted as s, is where the rider makes a ride request or the driver relocates to. If a driver decides to wait at his/her current location or has accepted a trip in the same area, r equals s.

Drivers are more likely to relocate to locations with higher expected service prices. To capture this effect, we propose utility function (1). We assume that driver relocation decisions follow multinomial logistic models, with explanatory variables of locational

attractiveness $\beta_{0,s}$, relocation time t_{rs}, and locational prices ρ_s. Locational attractiveness indicates how a location is favored by drivers because of factors other than time and price, such as safety, rider density, and easiness of getting returning trips. Locational prices ρ_s represent the expected trip standard rates originated from s times origin-base surge multipliers determined by TNC. The modeling framework is flexible to incorporate more explanatory factors. The deterministic components of drivers' utility function are given in (1).

$$U_{rs} = \beta_{0,s} - \beta_1 t_{rs} + \beta_2 \rho_s \tag{1}$$

where:

U_{rs}: deterministic component of utility measure for a driver going from r to s;

β: utility function parameters (model input);

t_{rs}: equilibrium travel time from r to s;

ρ_s: locational price at s.

Utility function (1) describes the utility of drivers at location r when they make relocation decisions from r to s. Utility function (1) does not aim to capture the heterogeneity of drivers at location r nor reflect how much each driver will actually get paid, since supply and demand may not be balanced at each location and drivers may be matched with trips with different trip lengths. But when drivers make relocation decisions, they do not know the length of trips that they are going to be matched with by the TNC. In other words, drivers' revenue from the next trip is a random variable before they relocate. The expectation of drivers' revenue depends on the expectation of trip length and the origin-based surge multipliers of their relocation destinations. Therefore, for drivers, the relocation decision making is independent of the specific destination of the next trip. Instead, it will depend on the expected trip fares originated from the region a driver relocates to.

While drivers have the flexibility to relocate themselves to other locations, travelers typically have predefined travel origins and destinations. In this study, we assume the travel demand D_s is endogenously given but they can choose the travel modes between requesting TNC services and driving. At each location s ($\in S$), we start with a linear ride-sourcing demand function, as defined in (2), to calculate ride-sourcing demand d_s. Driving demand is $D_s - d_s$. We note that the linear demand function (2) is used to keep a clear focus of this paper and it does not restrict the applicability of our modeling and computational approach for more sophisticated demand models (see Appendix C.1).

$$d_s = D_s - b_s \rho_s, \rho_s \le D_s / b_s \tag{2}$$

where:

d_s: flow rate of riders requesting ride-sourcing service at location s;

D_s, b_s: total travel demand originated from s and slope of demand function (model input).

To calculate the ride-sourcing OD demand d_{sk}, we need to multiply distribution coefficient δ_{sk} with d_s. d_s is independent of destinations because it is the ride-sourcing demand aggregating all possible destinations. δ_{sk} will be influenced by destination characteristics, trip lengths, and other related parameters. This modeling strategy is widely adopted in the classic "four-step travel demand model" for transportation planning (McNally, 2007), in which travelers are modeled as making four distinct decisions: trip generation, destination choice, modal choice, and route choice. To facilitate modeling and computation, these four steps are typically treated separately. In this study, we focus on modeling how travelers choose between different travel modes and routes and consider the total trip generation D_s and trip destination choice δ_{sk} as exogenous parameters. Saying that, we note that traffic distribution factors can be endogenously determined within the proposed modeling framework based on the travel time (t_{sk}) and travel distance (l_{sk}) from s to k, as well as locational attractiveness at location k. The reason travel time/distance is a good proxy to spatial pricing is because ride-sourcing trip fares are typically determined by trip time and distance.[3] The longer the travel time/distance is for a destination k, the higher the prices riders need to pay. Therefore, riders will less likely to choose that destination. This effect can be directly modeled using combined distribution and assignment (CDA) model with utility function (3) of destination choice for riders, where b_0, b_1, b_2 are utility coefficients corresponding to locational attractiveness, travel time, and trip distance.

$$U_{sk} = b_{0,k} - b_1 t_{sk} - b_2 l_{sk} \tag{3}$$

The interactions between drivers, riders, and other passenger vehicles will endogenously determine the mobility of the transportation system. We extend the combined distribution and assignment (CDA) model (Wilson, 1969) to describe the interactions

[3] https://help.uber.com/riders/article/how-are-fares-calculated/?nodeId=d2d43bbc-f4bb-4882-b8bb-4bd8acf03a9d.

between drivers' relocation and the routing of all ride-sourcing vehicles and conventional passenger vehicles. The model is described in (4).

$$\underset{\hat{\boldsymbol{v}},\check{\boldsymbol{v}},\boldsymbol{q}\in\mathbb{R}_+}{\text{minimize}} \quad \sum_{a\in\mathcal{A}}\int_0^{v_a} t_a(v_a)\mathrm{d}u + \frac{1}{\beta_1}\sum_{r\in\mathcal{R}}\sum_{s\in\mathcal{S}} q_{rs}\left(\ln q_{rs} - 1 - \beta_2\rho_s - \beta_{0,s}\right) \tag{4a}$$

subject to

$$\boldsymbol{v} = \sum_{r\in\mathcal{R},s\in\mathcal{S}} \hat{\boldsymbol{v}}_{rs} + \sum_{s\in\mathcal{S},k\in\mathcal{K}} \check{\boldsymbol{v}}_{sk}, \tag{4b}$$

$$(\hat{\lambda}_{rs}) \qquad A\hat{\boldsymbol{v}}_{rs} = q_{rs}E_{rs},\ \forall r,s \tag{4c}$$

$$(\check{\lambda}_{sk}) \qquad A\check{\boldsymbol{v}}_{sk} = \delta_{sk}D_sE_{sk},\ \forall s,k \tag{4d}$$

$$(\gamma_r) \qquad \sum_{s\in\mathcal{S}} q_{rs} = Q_r,\ \forall r \tag{4e}$$

where:

$\hat{\boldsymbol{v}}_{rs}, \check{\boldsymbol{v}}_{sk}$: link flow vector (each row corresponds to a link, a) grouped by OD for drivers and passenger vehicles, respectively;

$\boldsymbol{q}$: drivers' relocation flow vector (each row corresponds to an OD, rs);

v_a: aggregate traffic flow on link a;

$t_a(\cdot)$: travel time function of link a;

A: node-link incidence matrix of network, with 1 at starting node and -1 at ending node;

E_{rs}: O-D incidence vector of O-D pair rs with 1 at origin r, -1 at destination s. If $r = s$, $E_{rs} = \mathbf{0}$;

δ_{sk}: traffic distribution factor from s to k (model input);

Q_r: drivers initial availability at r;

$\check{\lambda}, \hat{\lambda}, \gamma, \eta$: dual variables of the corresponding constraints.

In the objective function (4a), the first term corresponds to the travel cost as modeled in a classic static user equilibrium model (Beckmann et al., 1956), the second term involving $q^{rs}\ln q^{rs}$ corresponds to the entropy of trip distribution, and the remaining terms are constructed in such a way that the first order derivative of the Lagrangian function with respect to q_{rs} resembles the utility measure (1) of drivers. This objective function does not have an intuitive physical interpretation to the authors' best knowledge, but it guarantees the first Wardrop principle (Wardrop, 1952) and the multinomial logit location choice assumption being satisfied, as formally stated in Lemma 1.

Lemma 1 (*Combined Distribution and Assignment for Ride-Sourcing System*)**.** *The optimal solutions* $(\hat{\boldsymbol{v}}^*, \check{\boldsymbol{v}}^*, \boldsymbol{q}^*)$ *of problem* (4) *are the equilibrium solutions for Wardrop user equilibrium and the relocation choice of drivers with multinomial logit model* (1) *given spatial prices* $\boldsymbol{\rho}$.

Proof. See Appendix A. □

Constraint (4b) calculates the aggregate link flow v_a from the link flow associated with OD pairs rs and sk. Constraints (4c), (4d) are link-based formulations of flow conservation at each node for each OD pair. Note that in the flow conservation constraint (4d), we consider not only trips fulfilled by ride-sourcing services (d_s), but also trips fulfilled by driving $D_s - d_s$. The total traffic originating from node s will be D_s. The reason is that ride-sourcing traffic flow is (currently) a small proportion of the link flow and considering external traffic is important to estimate traffic congestion. We model available driver per unit time period at location r as flow rate Q_r as given, which will relocate to different destinations s with a flow rate q_{rs}, as specified in Constraint (4e). One can also extend model (4) to consider the network effects of rider's destination on the spatial distribution of available drivers, i.e., if a driver takes a rider from s to r, then thereafter the driver will be at r (see Appendix C.2). The equilibrium path travel time t_{rs} is reflected by $\hat{\lambda}_{rs}^{a_i} - \hat{\lambda}_{rs}^{a_j}$. For details, please see the proof of Lemma 1.

Note that there are two types of ride-sourcing traffic in model (4). The first type is due to relocation or deadheading trips (i.e. no passengers on board); the second type is after ride-sourcing vehicles pick up passengers, drivers will drive riders to the riders' destinations, in which case origin and destination are known. The first type of ride-sourcing trip is Q_r in constraint (4e), which does not have specific destinations. D_s includes the second type of ride-sourcing trips and other driving trips. We do not need to separate travel demand by ride-sourcing and driving in mode (4) because the OD travel demand of vehicle traffic from s to k is fixed, which typically can be estimated from classic travel demand models. Although rider demand d_s does not directly enter into the model (4), d_s is endogenously determined and implicitly influences the locational prices ρ_s when we solve the multi-agent optimization models simultaneously.

Our proposed model can be extended to model elastic drivers' supply Q_r as a function of prices using discrete choice models. To do that, one can add a dummy relocation destination node for drivers in the transportation network to represent that drivers may decide to quit the service for the studied time period due to extremely low spatial prices offered at the candidate relocation destinations. The price parameter at the added dummy node reflects the benchmark revenue drivers may earn or expect to earn using their time. This approach does not need to modify our modeling (e.g., model (4)) and computational strategies.

3.1.2. TNC behaviors

Due to the uncoordinated behaviors of a large number of drivers and riders, individual drivers and riders do not have market power and only respond to the spatial prices set by the TNC. The pricing decisions of a TNC will influence the traffic equilibrium solutions of (4) and rider demand (2), which forms a mathematical programming with equilibrium constraints (MPEC) problem.

In this paper, we only consider TNC using origin-based pricing to influence the spatial distribution of ride-sourcing demand and supply. Origin-based pricing is widely adopted by TNCs (Zuniga-Garcia et al., 2020). The trip origin determines the amount of surge pricing for a trip, instead of the driver's location or trip destination. When prices are surging, TNCs will charge riders in the surge zone a multiplier to standard rates. The income of drivers serving the trips originated from the surge zone also scales up by the surge multiplier. The origin-based prices ρ_s used in this manuscript can be interpreted as regular fares for expected trip length multiplied by origin-base surge multipliers. Note that as long as the expected prices paid to drivers and paid by riders are linearly related to ρ_s, distinguishing payments from/to riders/drivers does not impact the equilibrium outcomes. This is because the impact will be implicitly captured by the coefficients β_2 in the utility function (1) and b_s in the demand function (2).

The TNC decision-making can be modeled as a bi-level problem (5). We assume that only one TNC in our study area, who would like to minimize the imbalance between supply and demand (see, objective (5a))[4], which has the advantage of improving driver/rider satisfaction and ultimately leads to long-term sustainable development and profits. A comparison between different objectives (minimizing imbalance versus maximizing short-term profits) will be presented in Section 5. Constraint (5b) calculates the imbalance as the difference between the flow of riders requesting services d_s and the number of drivers arriving at this location $\sum_{r\in\mathcal{R}} q_{rs}$. Calculation of traffic equilibrium patterns q_{rs} and ride-sourcing demand d_s are included in constraint (5c).

$$\underset{\rho\in\mathbb{R}^S}{\text{minimize}} \quad \sum_{s\in S} m_s \tag{5a}$$

subject to

$$m_s = |\sum_{r\in\mathcal{R}} q_{rs} - d_s|, \ \forall s \tag{5b}$$

$$(4), (2) \tag{5c}$$

where:

m^s : demand–supply imbalance at s.

While constraint (5b) can be reformulated as linear constraints, the bi-level structure still makes the whole problem challenging to solve to global optimal (Yang and H. Bell, 1998; Sinha et al., 2017). In Section 4, we propose an equivalent single-level convex reformulation of (5), which can be efficiently solved by commercial nonlinear solvers (e.g. IPOPT (Wächter, 2009)).

3.2. Mathematical modeling: Considering waiting time

In this section, we explicitly model the impacts of waiting time. Waiting time could influence the relocation decisions of drivers and the mode choices of riders. From an individual perspective, waiting time is heterogeneous and uncertain for each driver and rider. In this paper, we focus on the aggregated behaviors of drivers/riders and use expected waiting time to reflect the time costs to provide or receive services in a zone on average.

In reality, there are two phases, "matching" and "pick-up" after a ride request is made. For transportation system modeling purposes, Cobb–Douglas-type aggregate matching functions are widely adopted (Yang and Yang, 2011; Zha et al., 2016) to estimate the "meeting" rate and total waiting time (Li et al., 2021a). This modeling strategy is validated in Zha et al. (2016) using an agent-based simulation study. To consider different matching technologies (e.g., matching radius and matching time interval), a general matching function has been proposed for both single-interval optimization (Yang et al., 2020) and stationary analyses (Li et al., 2021a), which includes Cobb–Douglas-type matching functions as a special case. The main disadvantage of these studies is that there may not be a closed-form solution for the matching function and the waiting time could only be implicitly solved from a system of equations. Therefore, in this paper, we adopt a Cobb–Douglas matching function (see Eq. (6)) as a starting point to describe the total waiting time of drivers and riders, which includes waiting time in the matching phase and pick-up phase.

A Cobb–Douglas function is used mainly because of three reasons. First, the Cobb–Douglas function has a constant elasticity, which is specified by parameters α_1 and α_2. The elasticity can reflect the efficiency of the matching technology adopted by a ride-sourcing platform. Second, α_0 has a nice interpretation, which is related to the area of the matching zone and the cruising speed of

[4] Balancing supply and demand is the goal of dynamic pricing proposed by all TNC companies. See, for example, https://www.ridester.com/training/lessons/surge-primetime-boost-primezones/ (visited on Feb. 26, 2020).

vacant vehicles (Yang and Yang, 2011). Third, $\alpha_1 + \alpha_2$ is larger than, equal to, or smaller than one when the matching function is increasing, constant, or decreasing returns to scale. For a given area, it is typically assumed that $\alpha_1 + \alpha_2 > 1$ to represent increasing returns to scale of matching rate, because the increasing density of supply and/or demand will make it easier to match drivers with riders. Note that N_D and N_R are the number (instead of flow rate) of available drivers and awaited riders in a zone, which may change over our study time period due to a potential imbalance of supply and demand.

$$m(t) = \alpha_0 N_D^{\alpha_1}(t) N_R^{\alpha_2}(t) \tag{6}$$

Denote the locational average and total waiting time for drivers (D) and riders (R) as t_D, T_D, t_R, and T_R, respectively. Based on matching rate function (6), average waiting time for drivers D and riders R can be calculated in Eqs. (7),[5] where f_i ($i \in \{D, R\}$) is the flow rate of drivers/riders (i.e., $f_{D,s} = \sum_{r \in R} q_{rs}$, $f_{R,s} = d_s$) and T is the study period. Note that (7) is location specific, but we omit the location index s for all of the variables in (7) for notation conciseness.

$$\dot{N}_i(t) = f_i - m(t) = f_i - \alpha_0 N_D^{\alpha_1}(t) N_R^{\alpha_2}(t), \tag{7a}$$

$$T_i = \int_0^T N_i(t)dt, \ \forall i \in \{D, R\} \tag{7b}$$

$$t_i = \frac{T_i}{f_i T} = \frac{\int_0^T N_i(t)dt}{f_i T}, \tag{7c}$$

Eq. (7a) calculates the change rate of N_D (i.e. $\dot{N}_D$) as how many drivers relocate to s (i.e., $\sum_{r \in R} q_{rs}$) minus matching rate m. Similarly, the changing rate of N_R (i.e., $\dot{N}_R$) is determined by rate of rider demand in s (i.e., d_s) minus matching rate m. Eqs. (7b) and (7c) calculate the total and average waiting time for drivers and riders over T, respectively.

In (Yang and Yang, 2011) and some other subsequent studies, the authors assume the number of available drivers and riders are stationary, which implies that the matching rate will always equal to drivers/riders arrival rate. In contrast, we only assume that the *arrival rates* of drivers and riders are stationary during our studied time period. In other words, the flow rate could be greater, equal, or even lower than the matching rate if there is a reasonable level of available drivers and riders at the beginning of the studied period. When the flow rate is higher (or lower) than the matching rate for a certain duration, the number of available drivers and riders will increase (or decrease) and the matching rate will increase (or decrease) based on Eq. (6). The reason for this relaxation is to have a more realistic representation of the real ride-sourcing market, where the matching rate is typically not constant and available drivers and riders may fluctuate during the studied period. Our proposed model can be easily degenerated to consider the case when matching rate equals to drivers/riders flow rate by specifying $f_i = m(t), \forall i \in \{D, R\}$ in Eq. (7a) so that $\dot{N}_i(t) = 0$.

While solving Eq. (7) analytically is challenging, t_i ($\forall i \in \{D, R\}$) can be solved numerically given f_D, f_R and boundary conditions $N_D(0), N_R(0)$. We then apply linear regression techniques to estimate the relationship between t_i and f_i, $\forall i \in \{D, R\}$. The reason we need to use regression techniques is that the relationship between t_i and f_i is not well documented in the literature. We select $\alpha_0 = 0.1, \alpha_1 = \alpha_2 = 0.6$ for our numerical simulation to generate a sequence of t_i and f_i following system dynamic Eqs. (7). With these data generated, a linear regression model is used to estimate the coefficients in (8). When $\alpha_0 = 0.1, \alpha_1 = \alpha_2 = 0.6$, we have $a_0 = 6.29, a_1 = 2.24, a_2 = -2.40$ as least square estimators. $|a_2| > |a_1|$ implies that if both drivers and riders double their flow to a region, the waiting time for drivers and riders on average will be reduced (i.e., increasing return of scale for matching rate). The linear regression data generation procedures and output summary are presented in Appendix B.

$$t_i = a_0 f_i^{a_1} f_{-i}^{a_2} \quad \forall i \in \{D, R\} \tag{8}$$

Remark. Our modeling framework can have an equation similar to Eq. (6) to explicitly model the pickup time at a given zone, i.e., $t^{pickup}(t) = \alpha_0^{pickup} N_D^{\alpha_1^{pickup}}(t) N_R^{\alpha_2^{pickup}}(t)$. Since the pickup time could change over time, we can estimate the average pickup time over the studied time period as $\bar{t}^{pickup} = \frac{\int_0^T t^{pickup}(t)\mathrm{d}t}{T}$. In this case, the total waiting time (t_i^{total}) the drivers or the riders spend from placing ride requests to being picked up equates to $\bar{t}^{pickup} + t_i$. Following the same strategies to estimate the matching time t_i (i.e., Eqs. (7) and (8), we can estimate the relationship between the average pickup time $\bar{t}^{pickup}$ and drivers/riders flow f_R and f_D using regression techniques. Note that this extension does not affect the proposed computational strategies below.

To incorporate waiting time in a unified CDA framework, we define an augmented transportation network, $\bar{\mathcal{G}} = (\bar{\mathcal{N}}, \bar{\mathcal{A}})$. The augmenting procedures from $\mathcal{G}$ to $\bar{\mathcal{G}}$ is illustrated in Fig. 1 using a three-node transportation network, which has one driver node (node 1) and two rider nodes (node 2 and 3). For each rider node s in Fig. 1(a), we created s, s', and s'', representing nodes for markets, connectors, riders, respectively, with directed links connecting between them as shown in Fig. 1(b),[6]. In augmented network $\bar{\mathcal{G}}$, link flow $f_{s's}$, $f_{s''s}$ and $f_{s''s'}$ represent the flow of driver supply, rider demand, and travelers choosing to drive at node s, while the link cost $t_{s's}$ and $t_{s''s}$ are the waiting time for drivers ($t_{D,s}$) and riders ($t_{R,s}$), respectively. If travelers choose to drive, there is no waiting time, so that link cost $t_{s''s'} = 0$. In this paper, we do not consider cross-node matching. This is because we assume that each node represents a relatively large area (e.g., zipcode/city) where the majority of matching is within the node. However, the

[5] Eq. (7) is explained graphically in Appendix B.

[6] From Fig. 1 we can see that ignoring waiting time is a special case of considering waiting time when $a_0 = 0$ in (8), which makes link cost $t_{D,2}, t_{R,2}, t_{D,3}, t_{R,3} = 0$ in Fig. 1(b). This makes Fig. 1(b) identical as Fig. 1(a).

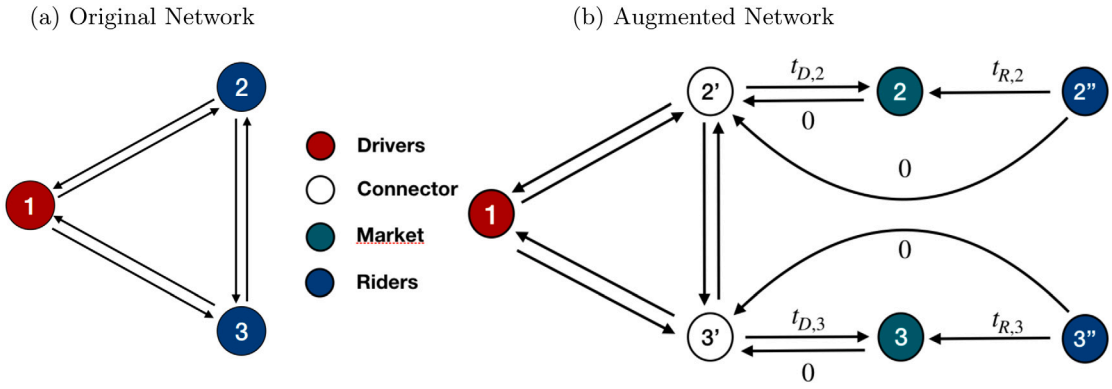

Fig. 1. Illustration of Network Augmentation.

augmented network (Fig. 1) can be further extended to consider the cross-node matching by adding single directional arrow from $2'$ to 3 and from $3'$ to 2. The "travel time" on these links represents the cross-node waiting time.

With an augmented network $\bar{\mathcal{G}}$, the utility function of drivers is identical with (1). Note that t_{rs} in (1) will include not only the travel time from r to s', $t_{rs'}$, but also the waiting time at s, $t_{s's}$. The drivers relocation and routing behaviors, therefore, can be modeled as (4) (replacing $\mathcal{G}$ with $\bar{\mathcal{G}}$), given spatial pricing $\boldsymbol{\rho}$.

For travelers at location s, the ride requesting demand function is not only dependent on the prices ρ_s, but also depends on the waiting time, $t_{s''s}$. We formulate the choice of ride-sourcing over driving using a binary logit model, with ride-sourcing utility function (9),

$$U_{s''s} = \beta'_{0,s} - \beta'_1 t_{s''s} - \beta'_2 \rho_s \tag{9}$$

where $\beta'_{0,s}, \beta'_1, \beta'_2$ are the utility coefficients for ride-sourcing attractiveness, waiting time, and ride-sourcing prices. Since the on-road travel time for driving and ride-sourcing are the same, travel time will be canceled out when travelers make mode choices and do not need to be included in (9). Note that the rider demand couples with waiting time (see (8) and (9)), we will formulate the travelers' mode choices using the CDA model in the augmented network $\bar{\mathcal{G}}$, where the destination s represents travelers choosing ride-sourcing services, and destination s' represents travelers choosing driving. The CDA model for riders' mode choice at each location s is shown in (10), where the first term corresponds to the conventional Wardrop user equilibrium, and the second term reflects the binomial logit choice between ride-sourcing and driving.

$$\underset{f_{R,s}\in\mathbb{R}_+}{\text{minimize}} \quad \int_0^{f_{R,s}} t_{R,s}(f_{D,s}, u)\mathrm{d}u + \frac{1}{\beta'_1}\left[f_{R,s}\left(\ln f_{R,s} - 1 + \beta'_2\rho_s - \beta'_{0,s}\right) + (D_s - f_{R,s})\left(\ln(D_s - f_{R,s}) - 1\right)\right] \tag{10}$$

Similar to formulation (5) for the "ignoring waiting time" case, the TNC decision making considering waiting time can be modeled as a bilevel problem, as shown in (11), where objective (5a) minimizes total demand–supply imbalance (calculated by (5b)), subject to drivers, riders, and all other travelers user equilibrium (4) and travelers' mode choices (10) in the augmented network $\bar{\mathcal{G}}$.

$$\underset{\boldsymbol{\rho}\in\mathbb{R}^S}{\text{minimize}} \quad \text{(5a)} \tag{11a}$$

subject to

$$\text{(5b)}, \text{(4)}, \text{replacing } \mathcal{G} \text{ with } \bar{\mathcal{G}}, \text{(10)} \tag{11b}$$

Remark. In this paper, we assume that travelers only choose between ride-sourcing and driving to keep a clear focus on the spatial pricing issues in ride-sourcing systems. However, we note that the proposed modeling framework can incorporate more sophisticated mode choice models. This can be seen from models (9) and (10), where riders choosing ride-sourcing or not (binary logit model) can be reformulated as a combined distribution and assignment (CDA) model. Since the CDA model can naturally consider more than two destinations (Florian et al., 1975), if other transportation modes are of interest, we can introduce dummy destination nodes in Fig. 1 to represent other travel modes and extend model (10) to solve for a multinomial logit model.

4. Solution approach

4.1. Solution approach: Ignoring waiting time

We start by showing that when problem (5) is solved to optimal, the ride-sourcing market will be balanced at each location. In addition, optimal solutions $\boldsymbol{\rho}^*$ is unique. This is more formally stated in Lemma 2.

Lemma 2 (*Balancing Ride Supply and Demand*). *ρ^* optimizes problem (5) if and only if ride supply and demand are balanced at each location given ρ^*. In addition, ρ^* is unique and $\rho_s^* \in [(D_s - \sum_{r\in R} Q_r)/b_s, D_s/b_s], \forall s \in S$.*

Proof. See Appendix A. □

Lemma 2 says that problem (5) is equivalent to the problem of finding the unique ρ^* that balances supply and demand at each location. Notice that ρ^* could be negative under extreme scenarios when too many available drivers exist in the system compared to rider demand. In other words, TNC may provide incentives for riders to use ride-sourcing services only when $D_s < \sum_{r\in R} Q_r$. However, this will not happen in reality given reasonable driver supply Q_r, since drivers will dynamically respond to extremely low prices (Bimpikis et al., 2019). On the other hand, based on Lemma 2, since $\rho_s^* \le D_s/b_s$, $d_s^* \ge 0$. In other words, d_s for all s cannot be negative in the optimal solution.

Leveraging Lemma 2, the optimal spatial prices can be obtained by solving a single-level convex optimization problem, which will be illustrated in the remainder of this section.

Problem (5) has three types of agents: drivers, riders, and TNC. Because of Lemma 2, the decision making of TNC can be reformulated as finding ρ^* such that

$$\sum_{r\in\mathcal{R}} q_{rs}^*(\rho^*) = D_s - b_s\rho_s^*, \forall s \in \mathcal{S} \tag{12}$$

where $q_{rs}^*(\rho^*)$ is the optimal solutions of (4) given ρ^*. This problem falls within the framework of multi-agent optimization problem with equilibrium constraints (MOPEC) (Ferris and Wets, 2013), where drivers make relocation decisions; riders decide whether to request ride-sourcing services; all travelers make route choices decisions; and the system is subject to equilibrium conditions (12). MOPEC has been applied in transportation, energy, economics domains, such as charging infrastructure planning (Guo et al., 2016b), hydro-thermal electricity systems optimization (Philpott et al., 2016), renewable energy supply chain planning (Guo and Fan, 2017), transportation and power system interdependence (Baghali et al., 2022; Guo et al., 2021), and computational Walrasian equilibrium (Deride et al., 2019).

Define two types of dummy agents in our problem, *Driver* and *Rider*. Given ρ, *Driver* solves problem (4), which determines the drivers relocation decision from r to s, $q_{rs}(\rho), \forall r, s$; and *Rider* solves problem (13), which determines the riders demand $d_s(\rho)$ at each location s. Note that problem (13) is a constructed unconstrained quadratic programming problem, which has a closed-form solution $d_s^*(\rho) = D_s - b_s\rho_s, \forall s \in \mathcal{S}$, identical to the demand function (2) we assumed.

$$\underset{d\in\mathbb{R}_+^S}{\text{minimize}} \quad \sum_{s\in\mathcal{S}} \frac{1}{b_s}[-D_s d_s + b_s\rho_s d_s + \frac{1}{2}(d_s)^2] \tag{13}$$

The equilibrium constraints (12) can be reformulated as (14).

$$\sum_{r\in\mathcal{R}} q_{rs}^*(\rho) = d_s^*(\rho), \forall s \in \mathcal{S} \tag{14}$$

We construct a single-level convex optimization problem (15), which will yield the same spatial pricing decisions as bilevel formulation, as stated in Theorem 1.

$$\underset{\hat{v},\hat{v},q,d\in\mathbb{R}_+}{\text{minimize}} \quad \frac{\beta_1}{\beta_2}\sum_{a\in\mathcal{A}}\int_0^{v_a} t_a(v_a)\mathrm{d}u + \frac{1}{\beta_2}\sum_{r\in\mathcal{R}}\sum_{s\in\mathcal{S}} q_{rs}\left(\ln q_{rs} - 1 - \beta_{0,s}\right) + \sum_{s\in\mathcal{S}}\frac{1}{b_s}\left(\frac{d_s^2}{2} - D_s d_s\right) \tag{15a}$$

subject to

$$(4b) \sim (4e)$$

$$(\rho_s) \quad \sum_{r\in\mathcal{R}} q_{rs} = d_s, \ \forall s \tag{15b}$$

The objective function (15a) is a combination of scaled objective functions (13) and (4a) without $\sum_{r\in\mathcal{R}} \rho_s q_{rs}$ and $\rho_s d_s$ terms. The purpose of scaling (13) and (4a) is to convert the units of both objective functions into monetary units so that they are addable. In addition, the optimal dual variables ρ_s^* of constraints (15b) will have a monetary unit in dollars and balance supply and demand at each location. Therefore, ρ^* can be interpreted as spatial prices to solve problem (5) based on Lemma 2.

Theorem 1 (*Single-Level Convex Reformulation*). *ρ solves bi-level problem (5) if and only if ρ is the optimal dual variable corresponding to constraint (15b) in single-level problem (15).*

Proof. See Appendix A. □

Problem (15) is a non-linear convex problem, with a convex objective function and linear constraints. So it can be efficiently solved to global optimal by commercial nonlinear solvers, such as IPOPT. For extreme large-scale problems, this reformulation opens up opportunities to apply classic and efficient transportation network solution algorithms, such as the Frank–Wolfe algorithm (Sheffi, 1985) and Evans' procedure (Evans, 1976). In this paper, we focus on small/medium transportation networks to draw policy insights and leave the development of advanced algorithms for extremely large networks for the future.

4.2. Solution approach: Considering waiting time

Directly solving TNC upper-level problem (11) is challenging due to non-convexity. We restate (11) as a problem of finding a maxinf-point for a bivariate function (bi-function) $W(\boldsymbol{\rho}, \boldsymbol{\phi})$, as shown in (16).

$$W(\boldsymbol{\rho}, \boldsymbol{\varphi}) = -\sum_{s \in S} \varphi_s \mathrm{ES}_s(\boldsymbol{\rho}), \quad \text{on } \mathbb{R}^S \times \Delta_S \tag{16}$$

where Δ_S corresponds to the S-dimensional unit simplex. ES_s is the square of demand–supply imbalance, defined in (17).

$$\mathrm{ES}_s(\boldsymbol{\rho}) = \left[\sum_{r \in \mathcal{R}} q^*_{rs}(\boldsymbol{\rho}) - f^*_{R,s}(\boldsymbol{\rho})\right]^2, \ \forall s \in S \tag{17}$$

where q^*_{rs} and $f^*_{R,s}$ are the optimal solutions (as a function of $\boldsymbol{\rho}$) of problem (4), replacing $\mathcal{G}$ with $\bar{\mathcal{G}}$) and ((10), respectively.

The relationship between maxinf point of $W(\boldsymbol{\rho}, \boldsymbol{\varphi})$ and the equilibrium spatial prices is stated in Lemma 3.

Lemma 3 (*Equilibrium Prices and Maxinf-Points*). *For $\boldsymbol{\rho} \in \mathbb{R}^S$, $\boldsymbol{\rho}$ is a maxinf-point of the Walrasian function W such that $W(\boldsymbol{\rho}, \cdot) \geq 0$, on Δ_S if and only if $\boldsymbol{\rho}$ is an equilibrium point.*

Proof. See Appendix A. □

This conversion is inspired by a theoretical development on lopsided convergence of bifunction by Jofré and Wets (2009), which offers the flexibility of constructing a sequence of approximate bifunctions with desired properties (including convexity and continuity) to solve for the original maxinf-point of $W(\boldsymbol{\rho}, \boldsymbol{\phi})$. A similar approach has been successfully implemented in (Guo et al., 2016b; Deride et al., 2019). In this paper, we highlight the key steps of the algorithm design.

Since $\inf_{\boldsymbol{\varphi}} W(\boldsymbol{\rho}, \boldsymbol{\varphi})$ lack of concavity in $\boldsymbol{\rho}$, we apply an *augmented Lagrangian* for this non-concave formulation. Given sequences of nonegative, nondecreasing scalars $\{r^\nu\}$, $\{M^\nu\}$, one can define a sequence of *augmented Walrasian* functions for this problem as shown in Eq. (18).

$$W^\nu(\boldsymbol{\rho}, \boldsymbol{\varphi}) = \inf_{\boldsymbol{z}} \left\{ W(\boldsymbol{\rho}, \boldsymbol{z}) + \frac{1}{2r^\nu} |\boldsymbol{z} - \boldsymbol{\varphi}|^2 | \boldsymbol{z} \in \Delta_S \right\}, \text{on } [\boldsymbol{\rho}^{\nu-1} - M^\nu, \boldsymbol{\rho}^{\nu-1} + M^\nu] \times \Delta_S \tag{18}$$

The idea of this procedure is to approximate the problem of finding maxinf-points of the original Walrasian function W, by computation of approximate maxinf-points $\boldsymbol{\rho}_\varepsilon$ (see Definition 1) given by a sequence of augmented Walrasians W^ν, which are easier to solve. Note that the proposed approach is not a heuristic approach since the convergence of the proposed approximation scheme is guaranteed, as stated in Theorem 2.

Definition 1 (*Approximating Equilibrium Point*). $\boldsymbol{\rho}_\varepsilon$ is an ε-approximating equilibrium point, denoted as $\varepsilon - \operatorname{argmaxinf} W$, for $\varepsilon \geq 0$, if the following inequality holds: $\left|\inf W(\boldsymbol{\rho}_\varepsilon, \cdot) - \operatorname{supinf} W\right| \leq \varepsilon$.

Theorem 2 (*Convergence of Approximating Maxinf-Points*). *Suppose that* $\operatorname{supinf} W$ *is finite. Consider non-negative sequences $\{r^\nu\}$, $\{M^\nu\}$, and $\{\varepsilon^\nu\}$ such that $r^\nu \nearrow \infty$, $M^\nu \nearrow \infty$, $\varepsilon^\nu \searrow 0$. Let $\{W^\nu\}$ be a family of augmented Walrasian functions associated with each parameters r^ν and M^ν. Let $\boldsymbol{\rho}^\nu \in \varepsilon^\nu - \operatorname{argmaxinf} W^\nu$, and $\boldsymbol{\rho}^*$ be any cluster point of $\{\boldsymbol{\rho}^\nu\}$. Then $\boldsymbol{\rho}^* \in \operatorname{argmaxinf} W$.*

Proof. See (Guo et al., 2016b). □

Following Theorem 2, we propose the computational algorithm, as summarized in Algorithm 1, to achieve a sequence of approximating maxinf-points.

Algorithm 1 Approximating Maxinf-Point Algorithm

Result: $\boldsymbol{\rho}^\nu$
initialization: $\nu = 0$, ε^0, M^0, r^0, gap^0, $\boldsymbol{\rho}^0$, ϵ, $0 < c_1 < 1$, $c_2 > 1$
while $\mathrm{gap}^\nu \geq \epsilon$ **do**
  Phase I: solve the minimization problem $\boldsymbol{\varphi}^{\nu+1} \in \operatorname{argmin} W^{\nu+1}(\boldsymbol{\rho}^\nu, \cdot)$
  Phase II: solve the maximization problem $\boldsymbol{\rho}^{\nu+1} \in \operatorname{argmax} W^{\nu+1}(\cdot, \boldsymbol{\varphi}^{\nu+1})$
  evaluate: $\mathrm{ES}_s(\boldsymbol{\rho}^{\nu+1}), s \in S$
  let: $gap^{\nu+1} = \max\{\mathrm{ES}_s(\boldsymbol{\rho}^{\nu+1}), s \in S\}$
  let: $\varepsilon^{\nu+1} = c_1 \varepsilon^\nu$, $M^{\nu+1} = c_2 M^\nu$, $r^{\nu+1} = c_2 r^\nu$
  let: $\nu := \nu + 1$
end

Phase I consists of the minimization of a quadratic objective function over the S-dimensional simplex. This can be solved using Cplex/Gurobi solver. Phase II is done without considering first-order information and relying on the BOBYQA algorithm (Powell, 2009), which performs a sequentially local quadratic fit of the objective functions, over box constraints, and solves it using a trust-region method. As $r^\nu \nearrow \infty$, and $M^\nu \nearrow \infty$, and $\varepsilon^\nu \searrow 0$, in virtue of Theorem 2, $\boldsymbol{\rho}^\nu \to \boldsymbol{\rho}^*$, a maxinf-point of W.

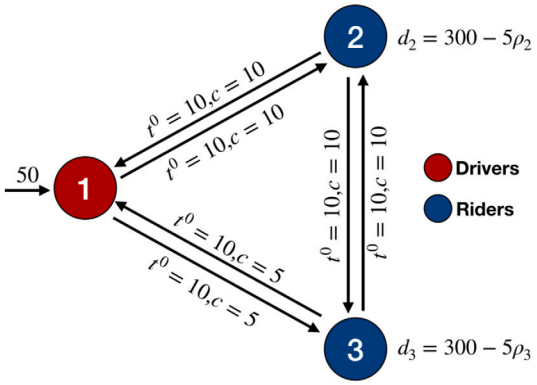

Fig. 2. Three Nodes Test Network.

Remarks.

1. The network augmenting procedures proposed in Section 3.2 result in a transportation network with a non-separable link-cost function (i.e., t_D and t_R), and the Jacobian of link-cost function is asymmetric, for which there is no known mathematical program whose solutions are the equilibrium flow pattern (Sheffi, 1985). But, the traffic equilibrium solutions can be achieved by the diagonalization method (Sheffi, 1985). We note that since the Jacobian of the link-cost functions is not positive definite when $|a_1| \leq |a_2|$ and $f_{D,s} \approx f_{R,s}$, the convergence of traffic equilibrium is not guaranteed in theory, although the algorithm may still convergence when this condition is violated (Fisk and Nguyen, 1982). To make our algorithm robust to the non-convergence of traffic equilibrium, the algorithm (Algorithm 1) we develop here does not require convergence for every iteration.

2. Notice that problem (11) has at least $|S|$ trivial equilibrium solutions, where only one location s attracts all the drivers $\sum_{r\in\mathcal{R}} Q_r$. This is because when driver supply approaches 0 and price is finite at one location, rider demand will also approach 0 due to infinite waiting time, and vice versa. The insight from this is that the ride-sourcing market may need a critical mass of drivers and riders to sustain. In this paper, we only focus on non-trivial equilibrium.

5. Numerical examples

In this section, we test our models and solution approaches on a three-node system (Fig. 2) and Sioux Falls network (Fig. 7). We implement our model on Pyomo 5.6.6 (Hart et al., 2017). We solve the problems using IPOPT 3.12.13 (Wächter, 2009) for the "ignoring waiting time" case, and Cplex 12.8 & BOBYQA (in NLopt 2.4.2) for the "considering waiting time " case, both with 0.1% optimality gap. All the numerical experiments presented in this section were run on a 3.5 GHz Intel Core i5 processor with 8 GB of RAM memory, under Mac OS X operating system.

5.1. Three-node network

The three-node test instance (Fig. 2) has one driver node (node 1) and two demand nodes (nodes 2 and 3). 50 drivers decide where to pick up riders at node 1. $\beta_0 = 0, \beta_1 = 1, \beta_2 = 0.6$. The link travel time has a form of $t_a = t_a^0[1 + 0.15 * (v_a/c_a)^2]$, where t_a^0 is the free flow travel time and c_a is the link capacity parameter. The value of t_a^0 and c_a for each link are shown in Fig. 2. Notice that this test instance is symmetric except that links between nodes 1 and 3 have lower capacity than other links.

5.1.1. Ignoring waiting time

We assume both node 2 and 3 have a demand function of $d_s = 300 - 5\rho_s$. Solving this problem using our single-level reformulation (15), we have $\rho_2 = 53.5, \rho_3 = 56.5$. Notice that with these locational prices, the demand market at both nodes 2 and 3 are balanced. The difference between ρ_2 and ρ_3 is because of the link congestion between nodes 1 and 3. In other words, node 3 is more congested to travel to due to limited link capacity. This is because, in order to attract more drivers to pick up riders at node 3, TNC needs to offer a higher locational price. If TNC does not consider transportation congestion, the optimal locational prices are $\rho_2' = \rho_3' = 55.0$, which will lead to an unbalance of supply and demand on both demand nodes in reality. These optimal solutions are validated by applying global solver SCIP (Achterberg, 2009) directly on mixed-integer nonlinear programming (MINLP) reformulation of bi-level problem (5). Reformulating bi-level problem into MINLP is standard, so we omit the detailed procedures for conciseness. For the three-node example, our reformulation (15) can be solved by IPOPT in 0.1 s, while MINLP formulation takes SCIP 5.6 s to solve. Although both SCIP and IPOPT solve the problem for global optimal, MINLP formulation is sensitive to the selection of big-M parameters, which is a challenging issue for mixed integer programming with switching constraints (Guo et al., 2016a).

Because TNC aims to balance supply and demand, transportation congestion can be worse under spatial pricing. We compare two scenarios: surge pricing and uniform pricing. If we change from uniform pricing to surge pricing, the total travel time increases slightly from 1333 to 1336. The increase in total travel time is because TNC gives incentives (surge pricing) to drivers traveling

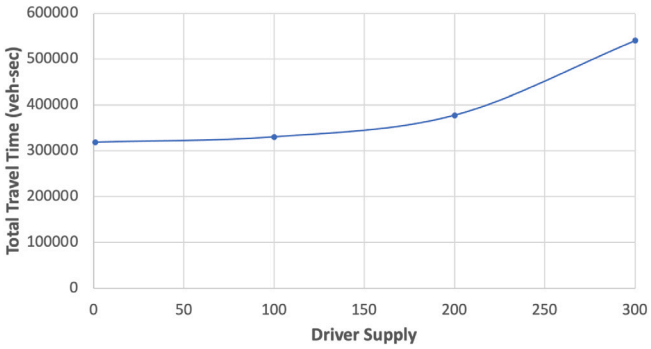

Fig. 3. Impact of Ride-sourcing Service on Traffic Congestion.

through congested areas in order to balance demand. This result matches the empirical findings in (Nie, 2017) that ride-sourcing may increase transportation congestion compared to taxi services. We also investigated the sensitivity of different ride-sourcing penetration levels on the total system travel time, as shown in Fig. 3. We can see that when the number of driver supply is at a low level compared to total travel demand, the impact of increasing ride-sourcing market share on total travel time is less significant. However, with the increasing driver supply, the system's total travel time increases non-linearly. The main reason is the additional relocation and pick-up VMT added to the transportation system in addition to the original traveler VMT. Regulations may be needed to prevent pricing selfishly by TNCs to improve overall transportation mobility, especially in congested areas.

Next, we compare the impacts of TNC's objectives between maximizing profits and minimizing imbalance. The problem of maximizing profits is shown in (19).

$$\underset{\rho\in\mathbb{R}^S}{\text{maximize}} \quad \sum_{s\in\mathcal{S}} \rho_s n_s \tag{19a}$$

subject to

$$n_s = \min\Big(\sum_{r\in\mathcal{R}} q^{rs}, D^s - b^s\rho_s\Big), \ \forall s \tag{19b}$$

$$(4) \tag{19c}$$

where:

n_s: : ride-sourcing matches at s.

(19a) maximizes total revenues. Since the majority of TNC operating costs go to marketing, administrative, and R&D,[7] which do not depend on the pricing decision variables. Therefore, the optimal pricing maximizes total revenues will also maximize total profits in the service territory. But we note that operating costs can be easily incorporated in (19a) if operating costs data is available. (19b) calculates the matches at each location s. For problem (19), we are not able to directly make the single-level reformulation as in (15). So we solve the bilevel problem (19) as MINLP using SCIP solver. The numerical results are shown in Figs. 4(a) and 4(b), in which we conduct sensitivity analyses of the total number of drivers Q_r and interception of demand function D_s on equilibrium prices with different TNC objectives. When TNC aims to minimize imbalance for each location, the optimal prices are almost linearly decreasing (increasing) with increasing supply (demand) for this toy test instance. The trend of optimal prices is slightly more complex when TNC aims to maximize profits. When supply is relatively high or demand is relatively low, TNC's profits are not restricted by drivers' availability, so TNC will set prices converging to monopoly prices, which are $D^s/2b^s, \forall s$. This means that when a TNC aims to maximize profits, the supply and demand may not necessarily be balanced at each location. This finding is consistent with the results in (Bimpikis et al., 2019) where endogenously determined spatial prices aiming to maximize profits may not always balance supply and demand. Notice that when demand is comparable to supply, prices minimizing imbalance of ride requests are identical with prices maximizing TNC profits, which indicates that maximizing balance of supply and demand leads to maximum profits for TNC.

5.1.2. Considering waiting time

When waiting time cannot be ignored for both drivers' and riders' decision making, we can solve problem (11) using Algorithm 1. We assume $D_s = 300, \ \forall s$. The riders' utility coefficients $\beta_0' = 0, \beta_1' = 1, \beta_2' = 0.6$.

With different initial locational prices, the convergence pattern of prices and ES are shown in Fig. 5. The average computation time is 27.8s, and all of the experiments converged efficiently to the same equilibrium solutions, $\rho_2^* = 37.4, \rho_3^* = 38.0, f_{D,2}^* = f_{R,2}^* = 33.1, f_{D,3}^* = f_{R,3}^* = 16.9$. Notice that TNC offers a slightly higher price at location 3, which is more congested to travel to. This observation is consistent with the observation in the "ignoring waiting time" case.

[7] https://news.crunchbase.com/news/understanding-uber-loses-money/.

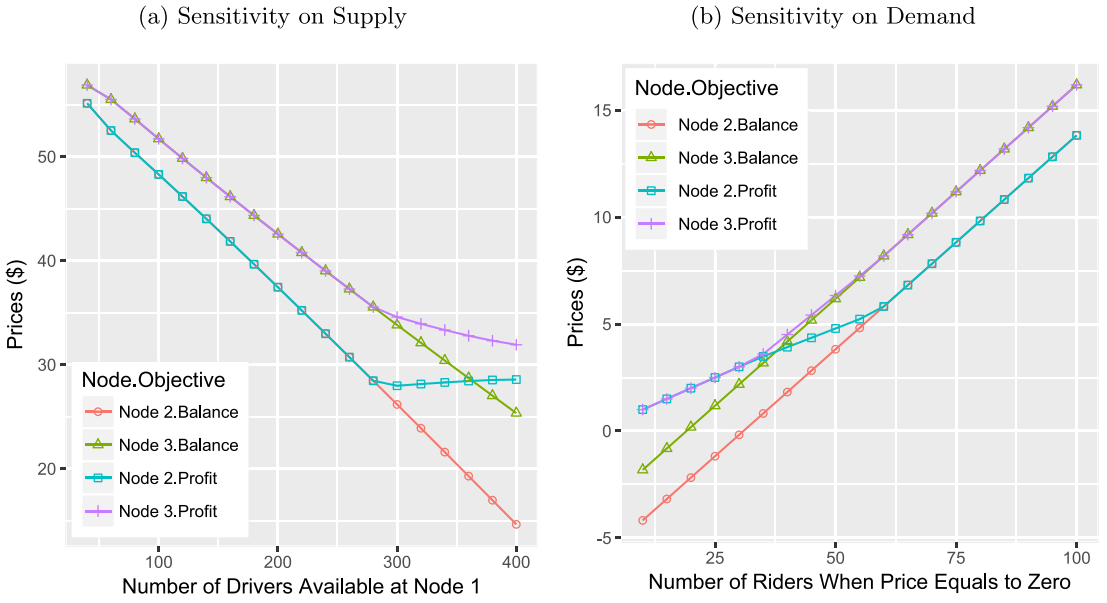

Fig. 4. Impacts of Supply and Demand on Optimal Surge Pricing.

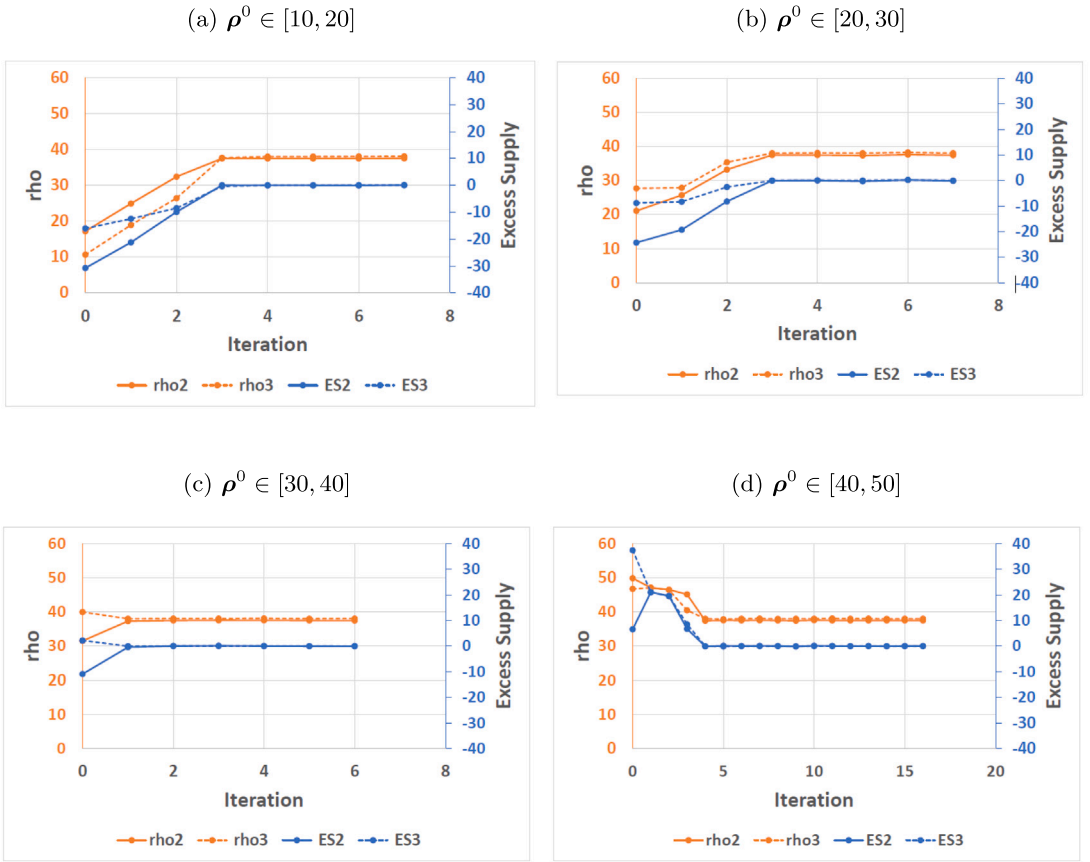

Fig. 5. Convergence Patterns with Different Starting Points ρ^0.

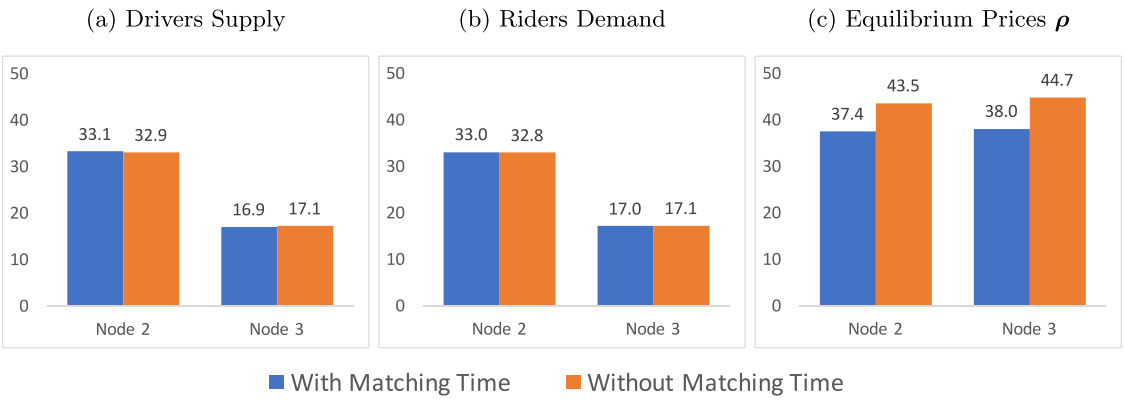

Fig. 6. Equilibrium Solutions For Ignoring and Considering Waiting Time Cases.

We compare the equilibrium solutions between the ignoring and considering waiting time cases, with the results of equilibrium spatial pricing, driver supply, and rider demand shown in Fig. 6. We can see that, compared to equilibrium prices, driver and rider flows are less sensitive to whether the waiting time is considered or not. The reason is that different locations have similar waiting times when supply and demand are balanced. For drivers, their relocation choices only depend on the utility difference between locations, which will not change if a similar waiting time is ignored. Therefore, driver supply remains unchanged (see Fig. 6(a)). Given the similar amount of driver supply, TNC will need to raise up locational prices (see Fig. 6(c)) to compensate for the ignored waiting time, so that rider demand still balances driver supply (see Fig. 6(b)).

5.2. Sioux Falls network

We implement our model using a medium-size test system, Sioux Falls network,[8] as shown in Fig. 7. In Fig. 7, the red and blue nodes (12 of each) represent the original locations of drivers and riders, respectively. Drivers supply at each red node is 50, while the demand function at each blue node is $d_s = 300 - 5\rho_s$. We adopt a 4th-order Bureau of Public Roads (BPR) function for link cost: $t_a = t_a^0[1 + 0.15 * (v_a/c_a)^4]$. Coefficients of utility function for base case (1) are $\beta_0 = 0, \beta_1 = 1, \beta_2 = 0.6$.

5.2.1. Ignoring waiting time

The optimal locational pricing decisions and total equilibrium travel time are shown in Fig. 8. With price sensitivity coefficient β_2 increase from 0.1 to 10, the price variances decrease (see Fig. 8(a)). This is because when drivers are more sensitive to prices, TNC needs a smaller price difference to attract drivers to the desired locations. At the same time, drivers are more willing to travel long distances to reach a location with higher prices. This will lead to higher system total travel time, as shown in Fig. 8(b).

SCIP is not able to solve the MINLP reformulation of problem (5) for Sioux Falls network, while IPOPT can efficiently solve (15) in 11.3, 6.1, and 4.9 s for $b_2 = 0.1$, 1, and 10, respectively.

5.2.2. Considering waiting time

Considering the waiting time, the problem can be solved by Algorithm 1 in 6.4 h, which is significantly longer than the computation time for the "ignoring waiting time" case. This is because of the lack of convexity for problem (11). But the algorithm converges reliably in 12 iterations, with convergence patterns of ES and ρ shown in Fig. 9.

Comparing the impact of spatial pricing on transportation congestion, the total travel cost is 3805.5 when spatial pricing is adopted, which is higher than a total travel cost of 3770.4 when TNC adopts uniform pricing. This observation is again consistent with the results in the "ignoring waiting time" case.

6. Discussion

In this paper, we have presented a new modeling framework and effective computational techniques for ride-sourcing spatial pricing problems, considering the leader–follower structure of TNCs, riders, and drivers in the peak traffic period. In the lower level, interactions between drivers' relocation, riders' mode choice, all travelers' routing behaviors, and network congestion are explicitly modeled. In the upper level, a single TNC provider optimally determines spatial prices to achieve its own objectives. When waiting

[8] Sioux Falls network consists of 24 nodes and 76 directed links. The number on each node/link in Fig. 7 is the node/link index.

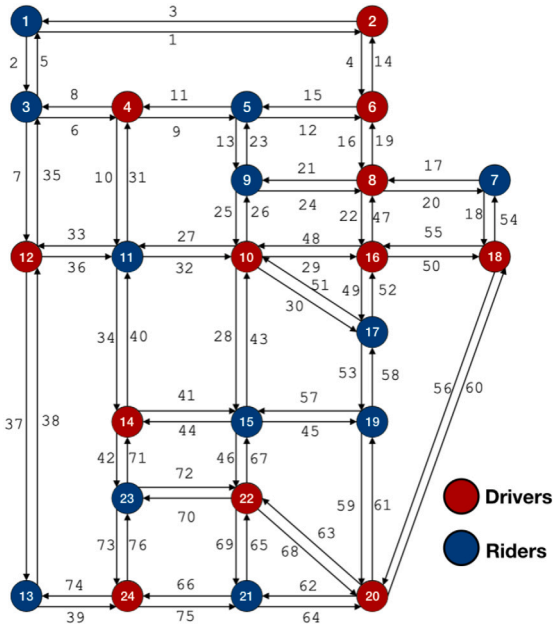

Fig. 7. Sioux Falls Test Network.

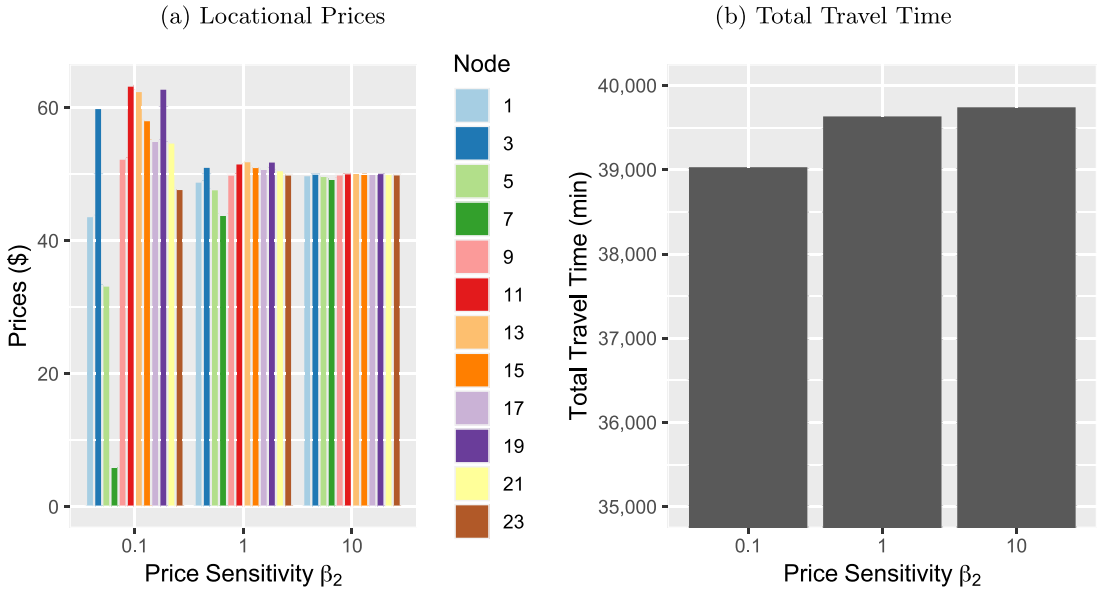

Fig. 8. Impacts of Supply and Demand on Optimal Surge Pricing.

time can be ignored, we show that the problem is equivalent to a convex optimization problem, which can be efficiently solved to global optimal by commercial nonlinear solvers. The existence and uniqueness of optimal solutions are proved. When waiting time cannot be ignored, we show that the lower-level drivers' and riders' two-sided interactions can be reformulated in a unified CDA framework with a non-separable link-cost function through network augmentation. The problem can be solved reliably by a lopsided convergence algorithm.

In addition to showing the effectiveness of our solution approaches, we demonstrated that (1) transportation congestion affects spatial pricing strategies, and spatial pricing strategies may aggravate transportation congestion compared to uniform pricing; (2) spatial pricing strategies that minimize supply–demand imbalance also maximize TNC profits when maximum demand and supply are comparable; (3) drivers' sensitivity to surge multipliers will significantly impact spatial prices and transportation congestion;

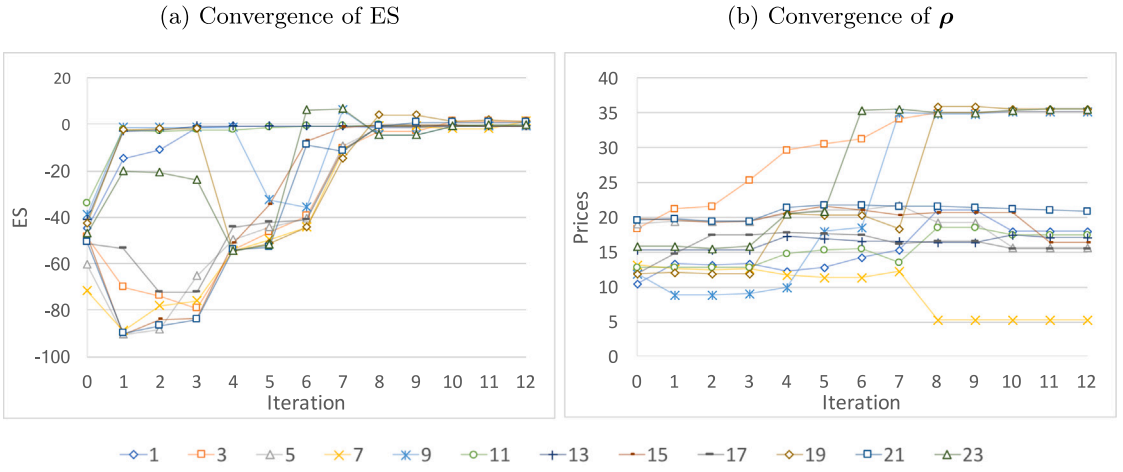

Fig. 9. Convergence of ES and ρ Considering Waiting Time.

and (4) the impacts of waiting time may be small on the distribution of drivers and riders but may be large on the scale of spatial pricing.

This research can be extended in several directions. From a methodological viewpoint, our model mainly focuses on spatial aspects. Coupling temporal and spatial dimensions are critical to fully understand the impacts of dynamic pricing on transportation systems. A spatial–temporal model will be needed to fully capture other important characteristics of the ride-sourcing system, such as (1) partitioning of driver-hours (driving time with riders, repositioning time, idle waiting time, and pick-up time) ; (2) network effects of riders destination and travel time on the spatial and temporal distribution of available drivers. In addition, several assumptions in this study can be relaxed. For example, the assumption on single TNC and inelastic total driver supply could be relaxed to generalize our findings. Our augmented network approach may be further extended to consider multiple TNCs by duplicating the "market" nodes in Fig. 1 to represent different service providers. However, single-level convex reformulation and equilibrium uniqueness may not be guaranteed. After gaining a clear understanding of the impacts of spatial pricing on transportation systems, strategies to mitigate the negative impacts from regulators' perspectives are urgently needed. Extending our model to a stochastic environment is another immediate next step considering the high level of uncertainties involved in the ride-sourcing market, such as congestion, rider demand, and driver supply. Although our model can be efficiently solved for small and medium transportation networks, algorithm development is needed for extremely large cases. Classic traffic assignment algorithm could be leveraged to solve the lower-level problem more efficiently. Solving a stochastic version of our model might also present further numerical challenges, for which decomposition methods (such as scenario decomposition and Benders decomposition) developed for stochastic programs may be integrated with the reformulation techniques in this study.

CRediT authorship contribution statement

Fatima Afifah: Formal analysis, Investigation, Writing – original draft, Writing – review & editing. **Zhaomiao Guo:** Conceptualization, Methodology, Writing – original draft, Supervision, Writing – review and editing.

Acknowledgments

This material is based upon work supported by the National Science Foundation under Grant No. 2041446.

Appendix A. Proofs.

Proof (Lemma 1). The proof of Lemma 1 is outlined as follows. Since (4a) is strictly convex (assuming $t_a(\cdot)$ is a strictly monotone increasing function) and constraints of model (4) are linear, Karush–Kuhn–Tucker (KKT) conditions are the sufficient and necessary optimality conditions, as shown in (A.1a)–(4b) and (A.1c) &–(4e), where a_i and a_j are starting and ending nodes of link a.

$$0 \le q_{rs} \perp \frac{1}{\beta_1}(\ln q_{rs} - \beta_2 \rho_s - \beta_{0,s}) + (\hat{\lambda}^r_{rs} - \hat{\lambda}^s_{rs}) - \gamma_r \ge 0 \tag{A.1a}$$

$$0 \le \hat{v}^a_{rs} \perp t_a(v_a) - \hat{\lambda}^{a_i}_{rs} + \hat{\lambda}^{a_j}_{rs} \ge 0 \tag{A.1b}$$

$$0 \le \check{v}^a_{rs} \perp t_a(v_a) - \check{\lambda}^{a_i}_{sk} + \check{\lambda}^{a_j}_{sk} \ge 0 \tag{A.1c}$$

(4b) – (4e)

We need to show that the KKT conditions (A.1) are equivalent to (i) the Wardrop equilibrium conditions (i.e., travel time in all routes actually used are equal and less than those that would be experienced by a single vehicle on any unused route) and (ii) logit model solutions. We outline the proofs of (i) and (ii) as follows.

Proof of (i): On one hand, for any path p connecting r and s with positive flow (i.e. $x_p > 0$), $\forall a \in p$, $\hat{v}^a_{rs} > 0$. Because of (A.1b), $t_a(v_a) = \hat{\lambda}^{a_i}_{rs} - \hat{\lambda}^{a_j}_{rs}$. Path travel time $\sum_{a\in p} t_a(v_a) = \hat{\lambda}^r_{rs} - \hat{\lambda}^s_{rs}$. On the other hand, for any path p' connecting r and s with zero flow (i.e. $x_{p'} = 0$), $\sum_{a\in p} t_a(v_a) \geq \hat{\lambda}^r_{rs} - \hat{\lambda}^s_{rs}$. Similarly, we can show the Wardrop equilibrium conditions for OD pairs s and k using (A.1c). Therefore, the traffic flows achieved by optimization problem (4) satisfy the Wardrop equilibrium conditions.

Proof of (ii): based on (A.1a), note that $q_{rs} > 0$, $\frac{1}{\beta_1}(\ln q_{rs} - \beta_2\rho_s - \beta_{0,s}) + (\hat{\lambda}^r_{rs} - \hat{\lambda}^s_{rs}) - \gamma_r = 0$, which means $q_{rs} = e^{\beta_{0,s} - \beta_1(\hat{\lambda}^r_{rs} - \hat{\lambda}^s_{rs}) + \beta_2\rho_s + \gamma_r} = e^{U_{rs}+\gamma_r}$. Because of (4e), $Q_r = \sum_{s\in S} q_{rs} = e^{\gamma_r}\sum_{s\in S} e^{U_{rs}}$. So $e^{\gamma_r} = \frac{1}{\sum_{s\in S} e^{U_{rs}}} Q_r$. We have $q_{rs} = \frac{e^{U_{rs}}}{\sum_{s\in S} e^{U_{rs}}} Q_r$, which follows the Logit model results. □

Proof (Lemma 2). Denote the optimized drivers distribution of model (4) as q^*_{rs}. Because of constraint (4e), the total driver supply is:

$$\sum_{r\in R}\sum_{s\in S} q^*_{rs} = \sum_{r\in R} Q_r \doteq \bar{Q},$$

which is a constant.

Because of constraint (5b), $m_s \leq \sum_{r\in R} q^*_{rs}$. Therefore, $\sum_{s\in S} m_s \leq \sum_{s\in S}\sum_{r\in R} q^*_{rs} = \bar{Q}$. Denote the optimal value of m_s as m^*_s, we have:

$$\sum_{s\in S} m^*_s \leq \bar{Q} \tag{A.2}$$

On the other hand,

$$\sum_{s\in S} m^*_s \geq 0 \tag{A.3}$$

The equality in (A.3) holds if and only if

$$\sum_{r\in R} q^*_{rs} = D_s - b_s\rho_s, \forall s \in S \tag{A.4}$$

In other words, we just need to show that $\exists \boldsymbol{\rho} \in \mathbb{R}^S$, s.t. (A.4) holds.

Define excess supply $ES^s(\boldsymbol{\rho}) = \sum_{r\in R} q^*_{rs}(\boldsymbol{\rho}) - (D_s - b_s\rho_s), \forall s$. Denote $\underline{\rho}^s = (D^s - \bar{Q})/b^s$ and $\bar{\rho}_s = D_s/b_s$. Define a convex compact set $H = \Pi_{s\in S}[\underline{\rho}_s, \bar{\rho}_s]$. We construct a function $\boldsymbol{\rho}' = h(\boldsymbol{\rho}) = (h_s(\rho_s), \forall s)$, such that:

$$\rho'_s = h_s(\rho_s) = \rho_s - \frac{(\bar{\rho}_s - \underline{\rho}_s)ES_s(\boldsymbol{\rho})}{\bar{Q}} = \rho_s - \frac{ES_s(\boldsymbol{\rho})}{b_s}, \rho_s \in [\underline{\rho}_s, \bar{\rho}_s]$$

We would like to show that $\rho'_s \in [\underline{\rho}_s, \bar{\rho}_s]$. Firstly, it can be easily seen that $h_k(\underline{\rho}_s) = \underline{\rho}_s - \frac{ES_s(\boldsymbol{\rho})}{b_s} = \underline{\rho}_s - \frac{\sum_{r\in R} q^*_{rs}(\boldsymbol{\rho}) - (D_s - b_s\underline{\rho}_s)}{b_s} \leq \frac{D_s - \bar{Q}}{b_s} - \frac{0-\bar{Q}}{b_s} = \bar{\rho}_s$, and $h_k(\bar{\rho}_s) = \bar{\rho}_s - \frac{ES_s(\boldsymbol{\rho})}{b_s} = \bar{\rho}_s - \frac{\sum_{r\in R} q^*_{rs}(\boldsymbol{\rho}) - (D_s - b_s\bar{\rho}_s)}{b_s} \geq \frac{D_s}{b_s} - \frac{(Q-0)}{b_s} = \underline{\rho}_s$. Secondly, we only need to show $h_s(\rho_s)$ is a monotone decreasing function. To show that, we take first order derivative of $h_s(\rho_s)$ with respect to ρ_s:

$$\dot{h}_s(\rho_s) = 1 - \frac{1}{b_s}\frac{\partial ES_s(\boldsymbol{\rho})}{\partial \rho_s} = 1 - \frac{1}{b_s}\left(\frac{\partial \sum_{r\in R} q^*_{rs}(\boldsymbol{\rho})}{\partial \rho_s} - \frac{\partial(D_s - b_s\rho_s)}{\partial \rho_s}\right)$$

Because $\frac{\partial \sum_{r\in R} q^{rs*}(\boldsymbol{\rho})}{\partial \rho^s} \geq 0$,

$$\dot{h}_s(\rho^s) \leq 1 - \frac{1}{b^s}(0 + b^s) = 0$$

Therefore, we have proved function $h(\cdot)$ is a mapping from H to H. In addition, because $h(\cdot)$ is monotone and continuous; and H is a convex compact subset of Euclidean space, based on Brouwer's fixed-point theorem, there exists $\boldsymbol{\rho}^* \in H$, such that $\boldsymbol{\rho}^* = h(\boldsymbol{\rho}^*)$. Therefore, for any s, $\exists \rho^*_s$ such that $\rho^*_s = \rho^*_s - \frac{ES_s(\rho^*)}{b^s}$, which leads to $ES_s(\boldsymbol{\rho}^*) = 0, \forall s$.

To show the uniqueness of $\boldsymbol{\rho}^*$, assuming that there exist $\boldsymbol{\rho}^{**}$ such that $ES_s(\boldsymbol{\rho}^{**}) = 0, \forall s$. Therefore, $h(\boldsymbol{\rho}^{**}) = \boldsymbol{\rho}^{**}$, i.e., $\boldsymbol{\rho}^{**}$ is another fixed point of $\boldsymbol{\rho}' = h(\boldsymbol{\rho})$. Without lost of generality, assuming $\rho^{**}_s > \rho^*_s$. Since $h_s(\cdot)$ is monotone decreasing, $\rho^{**}_s = h_s(\rho^{**}_s) \leq h_s(\rho^*_s) = \rho^*_s$, which is a contraction with the assumption that $\rho^{**}_s > \rho^*_s$. □

Proof (Theorem 1). Because problem (15), (4) and (13) are convex optimization, with convex and continuously differentiable objective function, closed and convex constraint sets, the optimal solutions to (15), (4) and (13) are equivalent to the solutions to certain variational inequalities (Nagurney and Siokos, 1997).

Denote the following items for notation conciseness.

- $\mathcal{X}$: constraint set (4b)–(4e);

- $\{\boldsymbol{x}, \boldsymbol{q}\}$: decision variables of model (4), where $\boldsymbol{x}$ include all the decision variables except $\boldsymbol{q}$;
- $f(\boldsymbol{x}, \boldsymbol{q})$: objective function of model (4) excluding $\sum_{r\in\mathcal{R}}\sum_{s\in S} q_{rs}\rho_s$. That is $f(\boldsymbol{x}, \boldsymbol{q}) = \frac{\beta_1}{\beta_2}\sum_{a\in\mathcal{A}}\int_0^{v_a} t_a(v_a)\mathrm{d}u + \frac{1}{\beta_2}\sum_{r\in\mathcal{R}}\sum_{s\in S} q_{rs}\left(\ln q_{rs} - 1 - \beta_{0,s}\right)$;
- $\{\boldsymbol{d}\}$: decision variables of model (13);
- $g(\boldsymbol{d})$: objective function of model (13) excluding $\sum_{s\in S}\rho_s d_s$. That is $g(\boldsymbol{d}) = \sum_{s\in S} 1/b_s[-D_s d_s + \frac{1}{2}(d_s)^2]$;

Following these notation, model (15) can be denoted as:

$$\min_{\boldsymbol{x},\boldsymbol{q},\boldsymbol{d}\geq 0} f(\boldsymbol{x}, \boldsymbol{q}) + g(\boldsymbol{d}),\ \text{s.t.}\{\boldsymbol{x}, \boldsymbol{q}\} \in \mathcal{X},\ \sum_{r\in\mathcal{R}} q_{rs} = d_s,\ \forall s$$

The equivalent variational inequalities for model (4), (13), (14) are shown in (A.5), (A.6), and (A.7), respectively.

$$\nabla_{\boldsymbol{x}} f(\boldsymbol{x}^*, \boldsymbol{q}^*)(\boldsymbol{x} - \boldsymbol{x}^*) + \nabla_{\boldsymbol{q}} f(\boldsymbol{x}^*, \boldsymbol{q}^*)(\boldsymbol{q} - \boldsymbol{q}^*) - \sum_{r,s}\rho_s^*(q_{rs} - q_{rs}^*) \geq 0,\ \forall \boldsymbol{x}, \boldsymbol{q} \in \mathcal{X},\ \boldsymbol{x}, \boldsymbol{q} \geq 0 \tag{A.5}$$

$$\nabla_{\boldsymbol{d}} g(\boldsymbol{d}^*)(\boldsymbol{d} - \boldsymbol{d}^*) + \sum_{s}\rho_s^*(d_s - d_s^*) \geq 0,\ \forall \boldsymbol{d} \geq 0 \tag{A.6}$$

$$(\sum_{r\in\mathcal{R}} q_{rs}^* - d_s^*)(\boldsymbol{\rho} - \boldsymbol{\rho}^*) \geq 0,\ \forall \boldsymbol{\rho} \tag{A.7}$$

On the other hand, model (15) can be solved by relaxing constraint (15b), whose KKT conditions are equivalent to VI (A.8).

$$\begin{aligned}&\nabla_{\boldsymbol{x}} f(\boldsymbol{x}^*, \boldsymbol{q}^*)(\boldsymbol{x} - \boldsymbol{x}^*) + \nabla_{\boldsymbol{q}} f(\boldsymbol{x}^*, \boldsymbol{q}^*)(\boldsymbol{q} - \boldsymbol{q}^*) + \nabla_{\boldsymbol{d}} g(\boldsymbol{d}^*)(\boldsymbol{d} - \boldsymbol{d}^*)\\ &\quad - \sum_{r,s}\rho_s^*(q_{rs} - q_{rs}^*) + \sum_{s}\rho_s^*(d_s - d_s^*) + (\sum_{r\in\mathcal{R}} q_{rs}^* - d_s^*)(\boldsymbol{\rho} - \boldsymbol{\rho}^*) \geq 0\\ &\qquad \forall \boldsymbol{x}, \boldsymbol{q} \in \mathcal{X},\ \boldsymbol{x}, \boldsymbol{q}, \boldsymbol{d} \geq 0\end{aligned} \tag{A.8}$$

Next, we just need to show that combining (A.5), (A.6), (A.7) is equivalent to (A.8). To show that, we will explain for any solutions satisfy (A.5), (A.6), (A.7), they also satisfy (A.8), and vice versa.

For solutions $(\boldsymbol{x}^*, \boldsymbol{q}^*, \boldsymbol{d}^*, \boldsymbol{\rho}^*)$ satisfying (A.5), (A.6), (A.7), they also satisfy (A.8) by combining VI (A.5), (A.6), (A.7). On the other hand, for $(\boldsymbol{x}^*, \boldsymbol{q}^*, \boldsymbol{d}^*, \boldsymbol{\rho}^*)$ satisfying (A.8), by selecting $\boldsymbol{d} = \boldsymbol{d}^*, \boldsymbol{\rho} = \boldsymbol{\rho}^*$, (A.8) becomes (A.5). Similarly, (A.6) and (A.7) are also satisfied.

Note that we do not derive VIs for the bilevel problem (5) when we prove Theorem 1. The reason why bilevel formulation (5) is equivalent to solving (4), (13), and (14) simultaneously is because of Lemma 2. In Lemma 2, we showed that the optimal pricing solutions to bilevel problem (5) are equivalent to market clearing prices for a single-level multi-agent optimization problem with (market) equilibrium constraints (MOPEC). The MOPEC problem considered here has two dummy decision makers: "drivers" (collectively) solve model (4), "riders" (collectively) solve model (13). And market is cleared by (14). In this MOPEC problem, all the decision makers are at the same level, i.e., there is no lower level decision makers but just equality market clearing constraints, so that each of model (4), (13), (14) can be written as VIs and be solved simultaneously. □

Proof (Lemma 3). On one hand, if ρ^* is a maxinf-point of the Walrasian with $W(\rho^*, \cdot) \geq 0$, it follows that for all unit vectors $e^s = (0, \ldots, 1, \ldots)$, the sth entry is 1, $W(\rho^*, e^s) \geq 0$ which implies $\mathrm{ES}_s(\rho^*) = 0$. On the other hand, if ρ^* is an equilibrium prices, i.e. $\mathrm{ES}_s(\rho^*) = 0$, it follows that $W(\rho^*, \cdot) = 0$. Because $W(\rho, \cdot) \leq 0$ for any ρ, ρ^* is a maxinf point of the Walrasian. □

Appendix B. Relationship between waiting time and driver/rider flow

Eq. (7) can be better explained graphically in Fig. B.10. Line 1 and 2 indicates the accumulative drivers (slope f_1) and riders (slope f_2) arrival curves, respectively. Line 3 represents the accumulative matching (with slope m calculated from Cobb–Douglas matching function). Fig. B.10 illustrates the case when the arrival rate of drivers f_1 is higher than riders f_2. We use waiting time for drivers t_1 as an example. The calculation process for waiting time of riders t_2 are similar. The area of the shaded region indicates the total delay of drivers T_1 till time period T, which can be numerically calculated based on Eq. (7b). Then, the average delay per driver (t_1) can be calculated based on Eq. (7c). By varying f_1 and f_2, we are able to generate a corresponding t_1 numerically, which will be used for estimating parameters in (8).

Following this data generation procedures outlined above, we randomly sample 10,000 pairs of f_1 and f_2 uniformly between $[0, 100]$ with a maximum difference of 10 and calculate t_1 and t_2. To use linear regression techniques, we take ln of both sides in Eq. (8) and estimate coefficients $\ln a_0$, a_1, and a_2 in $\ln t_i \sim \ln a_0 + a_1 \ln f_i + a_2 \ln f_{-i}$. A sample of data input for regression is summarized in Table B.1. The linear regression output is summarized in Table B.2.

Appendix C. Extensions

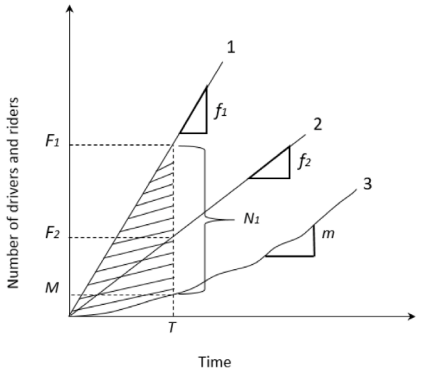

Fig. B.10. Graphical Representation of Waiting Time.

Table B.1
Sample regression input.

f1	f2	t1	t2	log_f1	log_f2	log_t1	log_t2
10	9	6.03	3.26	2.30	2.20	1.80	1.18
23	15	11.68	1.38	3.14	2.71	2.46	0.32
27	26	4.31	3.29	3.30	3.26	1.46	1.19
39	43	2.45	5.11	3.66	3.76	0.90	1.63
53	50	4.29	2.69	3.97	3.91	1.46	0.99
63	57	4.98	2.24	4.14	4.04	1.61	0.81
66	67	3.05	3.47	4.19	4.20	1.12	1.24
82	76	4.41	2.31	4.41	4.33	1.48	0.84
86	91	2.43	4.00	4.45	4.51	0.89	1.39

Table B.2
Regression summary output of (8).

SUMMARY OUTPUT

Regression Statistics	
Multiple R	0.95784929
R Square	0.91747526
Adjusted R S(	0.91745875
Standard Err(	0.04271119
Observations	10000

ANOVA

	df	*SS*	*MS*	*F*	*Significance F*
Regression	2	202.751098	101.375549	55571.218	0
Residual	9997	18.2369831	0.00182425		
Total	9999	220.988081			

	Coefficients	*tandard Erro*	*t Stat*	*P-value*	*Lower 95%*	*Upper 95%*
Intercept	1.84298058	0.00576574	319.643167	0	1.83167856	1.8542826
log_f1	2.24526358	0.00744279	301.669604	0	2.23067421	2.25985295
log_f2	-2.4035486	0.00748194	-321.24684	0	-2.4182147	-2.3888825

C.1. Extension of linear demand function

We note that the linear demand function (2) in Section 3.1 is used to keep a clear focus of this paper and it does not restrict the applicability of our modeling and computational approach for more sophisticated demand models. For example, one can adopt

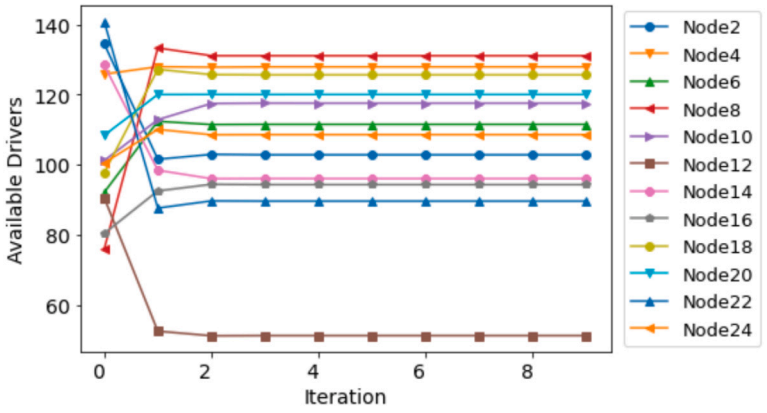

Fig. C.11. Convergence of Available Drivers Distribution.

nonlinear demand models, such as a logit model, to describe the ride-sourcing demand as a non-linear (decreasing) function of prices. We can choose a utility function of choosing ride-sourcing (with driving as the base option) as given in Eq. (C.1).

$$U_s = \beta'_{0,s} - \beta'_2 \rho_s \tag{C.1}$$

where $\beta'_{0,s}$ and β'_2 are the utility coefficients for ride-sourcing attractiveness and ride-sourcing prices at location s. The logistic demand model given utility function (C.1) can be derived in a closed-form expression as Eq. (C.2).

$$d_s = \frac{e^{U_s}}{1 + e^{U_s}} D_s \tag{C.2}$$

We can see that the overall modeling strategy for rider demand is the same for both the linear and nonlinear demand cases, i.e. Eqs. (2) and (C.2). We assume a total of D_s travelers choosing between ride-sourcing and driving. Prices are one of the key components influencing travelers' mode choices in both cases. Following these two models, within a total of travelers D_s, we can determine how many travelers choose ride-sourcing (denoted as d_s) and driving (denoted as $D_s - d_s$).

When rider utility of choosing ride-sourcing over driving is modeled using a logistic model and matching time can be ignored, i.e., model (C.1), the ride-sourcing demand at each location s, i.e., Eq. (C.2), can be obtained by solving a strictly convex optimization model (C.3), $\forall s$.

$$\underset{d_s \in \mathbb{R}_+}{\text{minimize}} \quad \left[d_s \left(\ln d_s - 1 + \beta'_2 \rho_s - \beta'_{0,s} \right) + (D_s - d_s) \left(\ln(D_s - d_s) - 1 \right) \right] \tag{C.3}$$

Following similar computational strategies as linear demand case (Section 4.1), when equilibrium prices $\boldsymbol{\rho}$ exist, model (5) (replacing linear demand function (2) with logistic model (C.2)) can be reformulated as model (C.4), which is a convex optimization problem.

$$\underset{\hat{\boldsymbol{v}}, \check{\boldsymbol{v}}, \boldsymbol{q}, \boldsymbol{d} \in \mathbb{R}_+}{\text{minimize}} \quad \frac{\beta_1}{\beta_2} \sum_{a \in \mathcal{A}} \int_0^{v_a} t_a(v_a) \mathrm{d}u + \frac{1}{\beta_2} \sum_{r \in \mathcal{R}} \sum_{s \in \mathcal{S}} q_{rs} \left(\ln q_{rs} - 1 - \beta_{0,s} \right) + \frac{1}{\beta'_2} \sum_{s \in \mathcal{S}} \left[d_s \left(\ln d_s - 1 - \beta'_{0,s} \right) + \beta'_2 (D_s - d_s) \left(\ln(D_s - d_s) - 1 \right) \right] \tag{C.4a}$$

subject to

$$\text{(4b)} \sim \text{(4e)}$$

$$(\rho_s) \qquad \sum_{r \in \mathcal{R}} q_{rs} = d_s, \ \forall s \tag{C.4b}$$

C.2. Extension of network effects of available drivers

In model (4), we treat spatial availability of drivers Q_r as exogenous variables. Exogenous vehicle fleet size assumption has also been made in (Zhou et al., 2021) to study ride-sourcing platform-integration. But the proposed model can also consider the network effects of the rider's destination on the spatial distribution of available drivers, i.e., if a driver takes a rider from s to r, then thereafter the driver will be at r.

Q_r not only depends on how many riders arrive at location r (denoted as d_r), but also depends on the rate of drivers start/end their service during the studied period (denoted as $Q_r^0 \in \mathbb{R}$). The flow rate of drivers available at location r can be calculated

in Eq. (C.5).

$$Q_r = d_r + Q_r^0 \tag{C.5}$$

Denote the proportion of riders going from s to r as δ_{sr} ($\sum_{r\in R}\delta_{sr} = 1$). d_r can be calculated in Eq. (C.6).

$$d_r = \sum_{s\in S}\delta_{sr}d_s \tag{C.6}$$

There are two approaches to consider the network effects within our modeling framework.

The first approach is an iterative approach. Because the formulation (4) and convex reformulation (15) are valid for any Q_r. We can recalculate Q_r iteratively by replacing d_r with the values from the last iteration. The equilibrium Q_r achieved in this way has incorporated the spatial distribution of riders' drop-off locations. The convergence of Q_r is shown in Fig. C.11 for Sioux Falls network example. We can see that within three iterations, the available drivers flow rate Q_r is stabilized for every location.

The second approach, we can add constraint (C.5) as a global constraint. Since we have proved Lemma 2 for any given $Q_r \in \mathbb{R}_+$, adding constraint (C.5) does not affect the existence and uniqueness of equilibrium prices and the convex reformulation thereafter. In addition, solving model (15) with additional global constraint (C.5) has minimum impact on the computational complexity since model (15) remains a convex optimization. After we solve for Q_r that satisfies condition (C.5), we can solve (15) separately with the equilibrium Q_r as input to get the corresponding dual variables ρ_s. The solution of Q_r following the second approach, i.e. adding global constraint of (C.5), is identical with the results from the first approach presented in Fig. C.11.

References

Achterberg, T., 2009. SCIP: Solving constraint integer programs. Math. Program. Comput. 1 (1), 1–41.

Alemi, F., Circella, G., Handy, S., Mokhtarian, P., 2018. What influences travelers to use Uber? Exploring the factors affecting the adoption of on-demand ride services in california. Travel Behav. Soc. 13, 88–104.

Baghali, S., Guo, Z., 2021. Impacts of privately owned electric vehicles on distribution system resilience: A multi-agent optimization approach. arXiv preprint arXiv:2105.03828.

Baghali, S., Guo, Z., Wei, W., Shahidehpour, M., 2022. Electric vehicles for distribution system load pickup under stressed conditions: a network equilibrium approach. IEEE Tran. Power Syst. 1–13.

Ban, X.J., Dessouky, M., Pang, J.-S., Fan, R., 2019. A general equilibrium model for transportation systems with e-hailing services and flow congestion. Transp. Res. B 129, 273–304.

Banerjee, S., Johari, R., Riquelme, C., 2015. Pricing in ride-sharing platforms: A queueing-theoretic approach. In: Proceedings of the Sixteenth ACM Conference on Economics and Computation. ACM, p. 639.

Battifarano, M., Qian, Z.S., 2019. Predicting real-time surge pricing of ride-sourcing companies. Transp. Res. C 107, 444–462.

Beckmann, M., McGuire, C., Winsten, C.B., 1956. Studies in the Economics of Transportation. Report.

Beojone, C.V., Geroliminis, N., 2021. On the inefficiency of ride-sourcing services towards urban congestion. Transp. Res. C 124, 102890.

Bimpikis, K., Candogan, O., Saban, D., 2019. Spatial pricing in ride-sharing networks. Oper. Res..

Cachon, G.P., Daniels, K.M., Lobel, R., 2017. The role of surge pricing on a service platform with self-scheduling capacity. Manuf. Serv. Oper. Manag. 19 (3), 368–384.

Camerer, C., Babcock, L., Loewenstein, G., Thaler, R., 1997. Labor supply of]New York city cabdrivers: One day at a time. Q. J. Econ. 112 (2), 407–441.

Castiglione, J., Cooper, D., Sana, B., Tischler, D., Chang, T., Erhardt, G.D., Roy, S., Chen, M., Mucci, A., 2018. TNCs & congestion.

Castillo, J.C., Knoepfle, D., Weyl, G., 2017. Surge pricing solves the wild goose chase. In: Proceedings of the 2017 ACM Conference on Economics and Computation. ACM, pp. 241–242.

Chen, L., Mislove, A., Wilson, C., 2015. Peeking beneath the hood of uber. In: Proceedings of the 2015 Internet Measurement Conference. ACM, pp. 495–508.

Chen, M.K., Sheldon, M., 2016. Dynamic pricing in a labor market: Surge pricing and flexible work on the uber platform. In: Ec. p. 455.

Chen, C., Yao, F., Mo, D., Zhu, J., Chen, X.M., 2021. Spatial-temporal pricing for ride-sourcing platform with reinforcement learning. Transp. Res. C 130, 103272.

Deride, J., Jofré, A., Wets, R.J., 2019. Solving deterministic and stochastic equilibrium problems via augmented walrasian. Comput. Econ. 53 (1), 315–342.

Dzisi, E.K., Ackaah, W., Aprimah, B.A., Adjei, E., 2020. Understanding demographics of ride-sourcing and the factors that underlie its use among young people. Sci. Afr. 7, e00288.

Evans, S.P., 1976. Derivation and analysis of some models for combining trip distribution and assignment. Transp. Res. 10 (1), 37–57.

Farber, H.S., 2005. Is tomorrow another day? The labor supply of New York city cabdrivers. J. Polit. Econ. 113 (1), 46–82.

Ferris, M.C., Wets, R., 2013. MOPEC: Multiple optimization problems with equilibrium constraints. URL http://pages.cs.wisc.edu/~ferris/talks/mopta-aug.pdf.

Fisk, C., Nguyen, S., 1982. Solution algorithms for network equilibrium models with asymmetric user costs. Transp. Sci. 16 (3), 361–381.

Florian, M., Nguyen, S., Ferland, J., 1975. On the combined distribution-assignment of traffic. Transp. Sci. 9 (1), 43–53.

Guda, H., Subramanian, U., 2019. Your uber is arriving: Managing on-demand workers through surge pricing, forecast communication, and worker incentives. Manage. Sci. 65 (5), 1995–2014.

Guo, Z., Afifah, F., Qi, J., Baghali, S., 2021. A stochastic multi-agent optimization framework for interdependent transportation and power system analyses. IEEE Trans. Transp. Electrification.

Guo, Z., Chen, R.L.-Y., Fan, N., Watson, J.-P., 2016a. Contingency-constrained unit commitment with intervening time for system adjustments. IEEE Trans. Power Syst. 32 (4), 3049–3059.

Guo, Z., Deride, J., Fan, Y., 2016b. Infrastructure planning for fast charging stations in a competitive market. Transp. Res. C 68, 215–227.

Guo, Z., Fan, Y., 2017. A stochastic multi-agent optimization model for energy infrastructure planning under uncertainty in an oligopolistic market. Netw. Spat. Econ. 17 (2), 581–609.

Gurvich, I., Lariviere, M., Moreno, A., 2019. Operations in the on-demand economy: Staffing services with self-scheduling capacity. In: Sharing Economy. Springer, pp. 249–278.

Hart, W.E., Laird, C.D., Watson, J.-P., Woodruff, D.L., Hackebeil, G.A., Nicholson, B.L., Siirola, J.D., 2017. Pyomo–Optimization Modeling in Python, Vol. 67, Second ed. Springer Science & Business Media.

He, F., Wang, X., Lin, X., Tang, X., 2018. Pricing and penalty/compensation strategies of a taxi-hailing platform. Transp. Res. C 86, 263–279.

Hu, B., Hu, M., Zhu, H., 2021. Surge pricing and two-sided temporal responses in ride hailing. Manuf. Serv. Oper. Manag..

Jofré, A., Wets, R.J.-B., 2009. Variational convergence of bivariate functions: Lopsided convergence. Math. Program. 116, 275–295.

Karamanis, R., Angeloudis, P., Sivakumar, A., Stettler, M., 2018. Dynamic pricing in one-sided autonomous ride-sourcing markets. In: 2018 21st International Conference on Intelligent Transportation Systems. ITSC, IEEE, pp. 3645–3650.
Lagos, R., 2000. An alternative approach to search frictions. J. Polit. Econ. 108 (5), 851–873.
Li, X., Ke, J., Yang, H., Wang, H., Zhou, Y., 2021a. A general matching function for ride-sourcing services. Available At SSRN 3915450.
Li, S., Yang, H., Poolla, K., Varaiya, P., 2021b. Spatial pricing in ride-sourcing markets under a congestion charge. Transp. Res. B 152, 18–45.
McNally, M.G., 2007. The Four-Step Model. Emerald Group Publishing Limited.
Nagurney, A., Siokos, S., 1997. Variational inequalities. In: Financial Networks. Springer, pp. 49–73.
Nie, Y.M., 2017. How can the taxi industry survive the tide of ridesourcing? Evidence from shenzhen, China. Transp. Res. C 79, 242–256.
Nourinejad, M., Ramezani, M., 2020. Ride-sourcing modeling and pricing in non-equilibrium two-sided markets. Transp. Res. B 132, 340–357.
NYCTLC, 2019. New York state's congestion surcharge. https://www1.nyc.gov/site/tlc/about/congestion-surcharge.page. (Accessed 15 February 2022).
Philpott, A., Ferris, M., Wets, R., 2016. Equilibrium, uncertainty and risk in hydro-thermal electricity systems. Math. Program. 157 (2), 483–513.
Pierog, K., 2019. Chicago approves traffic congestion tax on ride-hailing services. Reuters, 2019.
Powell, M., 2009. The BOBYQA Algorithm for Bound Constrained Optimization Without Derivatives. Cambridge NA Report NA2009/06, University of Cambridge, Cambridge.
Qian, X., Lei, T., Xue, J., Lei, Z., Ukkusuri, S.V., 2020. Impact of transportation network companies on urban congestion: Evidence from large-scale trajectory data. Sustainable Cities Soc. 55, 102053.
Rochet, J.-C., Tirole, J., 2006. Two-sided markets: A progress report. Rand J. Econ. 37 (3), 645–667.
Rysman, M., 2009. The economics of two-sided markets. J. Econ. Perspect. 23 (3), 125–143.
SAE international, 2018. Taxonomy and definitions for terms related to shared mobility and enabling technologies. SAE International, (J3163).
Sheffi, Y., 1985. Urban transportation networks: Equilibrium analysis with mathematical programming methods.
Sinha, A., Malo, P., Deb, K., 2017. A review on bilevel optimization: From classical to evolutionary approaches and applications. IEEE Trans. Evol. Comput. 22 (2), 276–295.
Tang, W., Wang, H., Wang, Y., Chen, C., Chen, X.M., 2022. A bi-level optimization model for ride-sourcing platform's spatial pricing strategy. J. Adv. Transp. 2022.
Taylor, T.A., 2018. On-demand service platforms. Manuf. Serv. Oper. Manag. 20 (4), 704–720.
Vignon, D.A., Yin, Y., Ke, J., 2021. Regulating ridesourcing services with product differentiation and congestion externality. Transp. Res. C 127, 103088.
Wächter, A., 2009. Short tutorial: getting started with ipopt in 90 minutes. In: Dagstuhl Seminar Proceedings. Schloss Dagstuhl-Leibniz-Zentrum für Informatik.
Wardrop, J.G., 1952. Some theoretical aspects of road traffic research. In: ICE Proceedings: Engineering Divisions, vol. 1. Thomas Telford, pp. 325–362.
Wilson, A.G., 1969. The use of entropy maximising models, in the theory of trip distribution, mode split and route split. J. Transp. Econ. Policy 108–126.
Yang, H., H. Bell, M.G., 1998. Models and algorithms for road network design: A review and some new developments. Transp. Rev. 18 (3), 257–278.
Yang, H., Leung, C.W., Wong, S., Bell, M.G., 2010. Equilibria of bilateral taxi–customer searching and meeting on networks. Transp. Res. B 44 (8–9), 1067–1083.
Yang, H., Qin, X., Ke, J., Ye, J., 2020. Optimizing matching time interval and matching radius in on-demand ride-sourcing markets. Transp. Res. B 131, 84–105.
Yang, H., Wong, S., 1998. A network model of urban taxi services. Transp. Res. B 32 (4), 235–246.
Yang, H., Yang, T., 2011. Equilibrium properties of taxi markets with search frictions. Transp. Res. B 45 (4), 696–713.
Zha, L., Yin, Y., Du, Y., 2018a. Surge pricing and labor supply in the ride-sourcing market. Transp. Res. B 117, 708–722. http://dx.doi.org/10.1016/j.trb.2017.09.010, URL http://www.sciencedirect.com/science/article/pii/S0191261517307683, TRB:ISTTT-22.
Zha, L., Yin, Y., Xu, Z., 2018b. Geometric matching and spatial pricing in ride-sourcing markets. Transp. Res. C 92, 58–75.
Zha, L., Yin, Y., Yang, H., 2016. Economic analysis of ride-sourcing markets. Transp. Res. C 71, 249–266.
Zhou, Y., Yang, H., Ke, J., Wang, H., Li, X., 2021. Competition and third-party platform-integration in ride-sourcing markets. Transp. Res. B.
Zuniga-Garcia, N., Tec, M., Scott, J.G., Ruiz-Juri, N., Machemehl, R.B., 2020. Evaluation of ride-sourcing search frictions and driver productivity: A spatial denoising approach. Transp. Res. C 110, 346–367.